Measuring circadian light through High Dynamic Range (HDR) photography

Bo Yun Jung

A thesis
submitted in partial fulfillment of the
requirements for the degree of

Master of Science in Architecture

University of Washington

2017

Committee:

Mehlika Inanici

Judith Heerwagen

Program Authorized to Offer Degree:

Architecture

University of Washington

Abstract

Measuring circadian light through High Dynamic Range (HDR) photography

Bo Yun Jung

Chair of the Supervisory Committee:
Associate Professor Mehlika Inanici
Department of Architecture

Human ocular system functions in a dual manner. While the most well know function is to facilitate vision, a growing body of research demonstrates its role in resetting the internal body clock to synchronize with the 24 hour daily cycle. The internal body clock in human beings is close to, but not equal to, 24 hour rhythms, and it requires environmental cues, such as timed light and dark cycles, to synchronize with the local time. Before the introduction of electrical lighting, human's patterns of light and dark exposures followed the natural diurnal cycles. In the modern days, this pattern changes drastically as 90% of adult human life is spent indoors and electric lighting prominently disturbs the nocturnal cycles.

With most research on circadian rhythm performed in controlled laboratory environments, little is known about the variability of circadian light within built and natural environment. Currently, very few specialized devices measure the circadian light which are not accessible to

many researchers and practitioners. Therefore, there is a need for accessible measurement devices.

In this thesis, calibration and validation procedures of High Dynamic Range (HDR) photography to measure circadian light is developed and tested. Accuracy of HDR photographs to measure photopic luminance have been previously validated. However, color accuracy of camera sensors hasn't been studied, and precise color information is required to accurately capture circadian light. In this thesis, camera color accuracy was evaluated through CIE trichromatic (XYZ) measurements; results demonstrated strong linear relationship between the camera recordings and scientific grade colorimeter. By applying simple correction, it is possible to correct color alignment, and therefore, to use HDR photographs to capture both photopic (lux and cd/m^2) and circadian lighting values (Equivalent Melanopic Lux, EML or Equivalent Melanopic cd/m^2). The developed technique and workflow has been used to capture outdoor and indoor scenes. Various examples illustrate the impact of architectural context, weather, view direction and spectra of light on circadian light exposure. Given data reduction in CIE XYZ measurements, full spectrum measurements were further collected to test validation of the methodology. Field and laboratory studies showed circadian light measurements from HDR Photographs corresponded to physical quantity of circadian luminance with reasonable precision and repeatability.

Acknowledgments

I would first like to thank Prof. Mehlika Inanici for all her guidance and patience through my Master's degree. Her enthusiasm and profound understanding in the subject of lighting has inspired me to dive deeper and explore different aspects of lighting design and research. She has been an incredible mentor whom I feel very fortunate to have met in my life. I also would like to thank her for all resources she provided for my thesis work; they were used to capture all the HDR photographs used in the thesis.

I thank my committee member, Judith Heerwagen, who graciously agreed to serve on my committee and provided timely feedback and support. Prof. Brian Johnson has encouraged me to start coding which saved a lot of time and effort throughout my thesis work. He has helped and guided me in many other ways during my degree, probably more than he realizes.

Prof. Chris Meek has given valuable advices throughout my studies and provided me the opportunity to work at Integrated Design Lab. I would also like to thank him for lending me the illuminance color meter which was used for my thesis. I also include Eric Stranberg

from lighting design lab in this acknowledgment for his generosity in lending the spectrophotometer, also used in my thesis.

Lastly, I would like to thank my friends and family. My good friends Dhara Mehta and Doaa Alsharif who often spent late evenings with me during quarters have been most dependable. I also thank Yunjae Lee for all his love and support despite the distance. Finally, I thank my parents for their enduring love and confidence in me. I am forever indebted to their support.

Table of Contents

List of Figures

1. Introduction

Circadian rhythm is cycle of physiological and neuroendocrine responses of living beings. With recent discovery of intrinsically photosensitive retinal ganglion cells (ipRGCs – 5th photoreceptor mediating circadian response) research on circadian rhythm is quickly evolving. Human circadian rhythm evolved in response to daylight as the primary light source. Today, light exposure pattern deviates greatly from natural light and dark cycle due to electric light and the built environments. Research shows this shift from biologically accustomed daylight exposure has serious impact in human health and wellbeing; short term disruption leading to sleep disorders and lower alertness. Long term affects are linked to increased likelihood for breast cancer, obesity, diabetes, depression, mood disorders and alzheimer's disease.[1][2][3] It is therefore crucial to study the effect of light in human circadian rhythm within luminous environment.

Most of current research has been performed in controlled laboratory environments leading to lack of data regarding variability of circadian light within the built and natural environments. Accessible measurement devices are needed to quantify quantity and variability of circadian light to advance research and its application within built environments. Availability of such data is crucial for architects and lighting designers to study the impact of their design decisions on circadian lighting, and develop guidelines for circadian friendly built environments.

The objective of this thesis is to develop and demonstrate calibration and validation procedures to measure circadian light through a commercially available camera. The concept of capturing

1

light using photography is not new. However, available photography techniques for scientific measurement of lighting mostly focus on photopic light and vision. This research is undertaken to develop the methodology and workflow to measure circadian light. Database of High Dynamic Range (HDR) images are collected along with colorimetric measurements (CIE XYZ) under varying spectra in indoor and outdoor spaces. This database is used to derive the color calibration functions for the camera, and the calibrated images are post processed to calculate the circadian light (Equivalent Melanopic Lux or cd/m^2). A user who has access to a camera, fisheye lens, and hand held colorimeter can follow the image capture and post processing procedures in this thesis to measure the circadian lighting in built and natural environments.

The thesis is organized in seven chapters. Literature review regarding research on circadian rhythms both in photobiology and in building sciences will be discussed in chapter 2 and 3. Chapter 4 describes method of post process and calibration of HDR photographs to measure circadian light. Calculated results from HDR photographs are shown in chapter 5 and chapter 6 discusses validation of the methodology. Finally, conclusions, contributions and future work is discussed in chapter 7.

2. Background - Findings from photobiology

This chapter discusses the current research on circadian rhythms to review current knowledge and identify gaps. Most of the scientific knowledge regarding the subject of circadian rhythm comes from photobiology. Although it is still in its premature state to provide a comprehensive understanding of its impact on humans, substantial body of knowledge has accumulated. This section explains the non-visual system and entrainment of the circadian system.

2.1. Visual and Non-visual system

A significant portion of knowledge accumulated about the human eye is related to its role on the visual system. The visual system is a complex system of network connected from the eye to the brain. Schematic summary of the visual pathway is shown in figure 2.1, beginning at the eye. Light is first received at the cornea and transmitted to the back of the eyeballs on the retina. In the retina, light stimulates photosensitive cells called rods and cones that send neural signals to the brain through the optic nerve. Rods are the active receptors in scotopic vision (in dark, non-color vision) and 3 different types of cones are the active receptors for photopic vision (in light, color vision). Rods and cones are located throughout the retina, but cones are concentrated around the fovea, while density of rods decline around the fovea. This means that human color vision is centred around the middle of the visual field. After rods and cones send electric signals to the optic nerve, signals are sent to the back of the brain called visual cortex in the cerebral hemispheres. This visual pathway facilitates how humans perceive shape, color, movement and even complex geometries such as faces from different angles.[4]

3
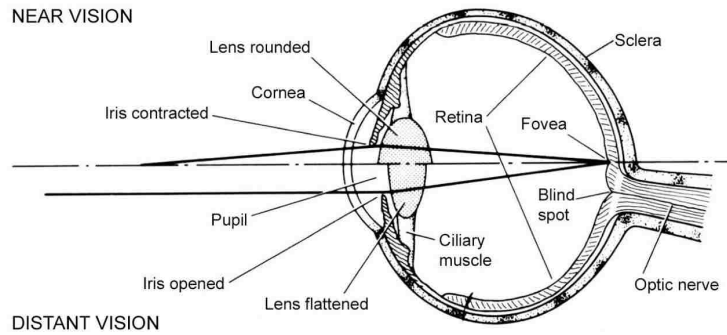
Figure 2.1. Human eye [5]
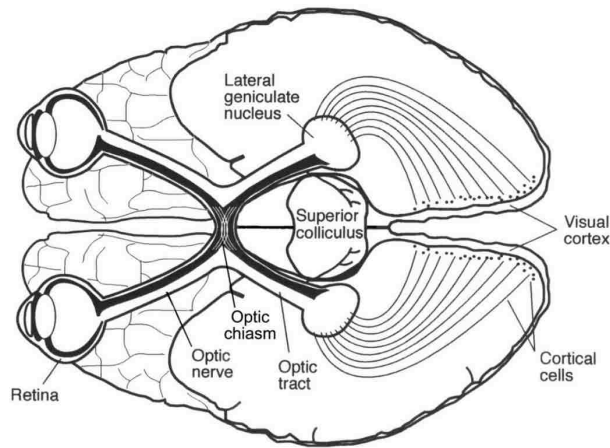
Figure 2.2. Visual pathway [5]

Contrary to the visual system which has been studied extensively for almost a century, non-visual system was only recently discovered when a 5th photosensitive cell was discovered in rodent retina called intrinsically photosensitive Retinal Ganglion Cells (ipRGCs).[6][7] These cells comprise of only 1-5 % of Retinal Ganglion Cells (RGC) and is located at the base of the retina.[8][9] Despite this small percentage, ipRGCs contains photopigment called melanopsin which is found throughout the entire ipRGC cell (dendrites, cell body and axons) which covers almost the entire

retina. ipRGCs have different properties to rods and cones. ipRGCs do not collect visual information from light but respond to irradiance levels. Having very narrow receptive field, ipRGCs are insensitive to rapid light changes and responds strongly to slow or still light for sustained periods.[10] It is also most sensitive to blue light at wavelengths around 480nm (rods and cones are most sensitive around green-blue and green respectively).[11] Further explanation on the spectra sensitivity of 5 different photoreceptors (rods, 3 cones, and ipRGCs) is described in section 2.2.
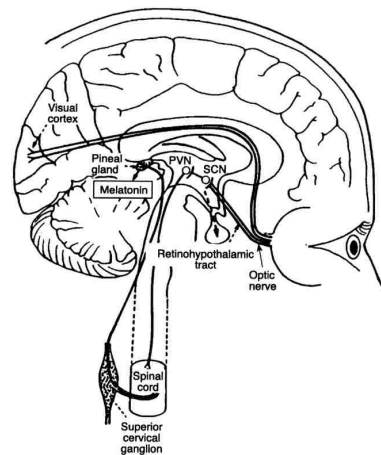
Figure 2.3. Non-visual pathway [5]

Most of the neural signals from the ipRGCs travel through a different pathway from the visual system, to the suprachiasmatic nuclei (SCN) via retinohypothalamic tract (RHT).[12] SCN is a cluster of neurons in hypothalamus located in middle of the brain and controls mammalian internal biological clock. In rats, it has been shown to saturate after certain amount of irradiance, unaffected by further light stimulus.[13] Moreover, it showed sustained response to continuous light for as long as 30 to 60 minutes.[14] This again shows that non-visual system is insensitive to rapid

5

changes of light and responds to sustained light exposure. To synchronize timing of physiological and behavioral activities within the body, SCN sends neural signals to various parts of the nervous system. This signal determines not only sleep patterns through melatonin secretion from pineal gland, but also core body temperature, blood pressure and changes in other hormone levels such as cortisol that are essential in regulating circadian rhythms. Full function of signals from ipRGCs not processed through SCN is not fully known yet. But it has been known to affect conventional visual process as well as pupillary light reflexes.
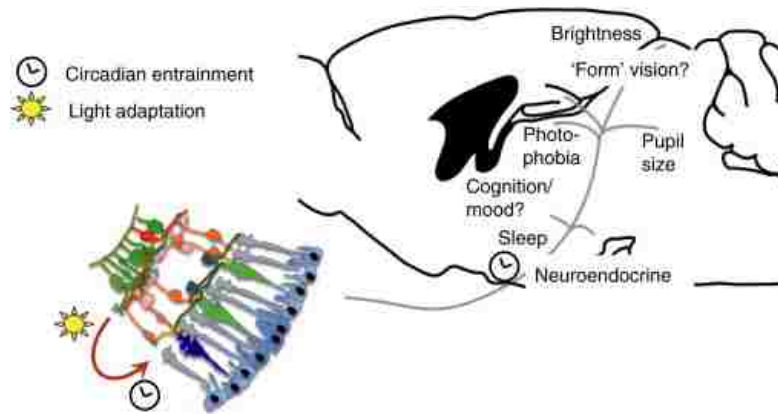
Figure 2.4. Various functions of ipRGCs [15]

2.2. Spectral Sensitivity Curve of five photoreceptors

Photoreceptors involved in visual and circadian pathway contain different photopigments. Each of these photopigments are sensitive to particular spectra of light. When photoreceptors receive enough stimuli (receive enough intensity of light corresponding to the photopigment's spectra sensitivity), it sends neural signals for visual or circadian neural processing. For the visual system, the photoreceptors are rods and cones. There are 3 types of cones; S, M, L which peaks around 450, 525 and 575 nm respectively.[16] Rods have peak spectral sensitivity around 500 nm. Average

6

spectral sensitivity curve of S, M, L cones is called photopic curve and represents visual sensitivity of the human eye. Spectral sensitivity curve of rods is excluded in the photopic curve as rods are mostly used for non-colored vision in dim conditions. The Commission Internationale de l'Éclairage (CIE) established a standard version of photopic curve based on psychophysical assessments of brightness for a standard observer. Known as luminous efficiency function or 1924 CIE standard photometric observer function, this curve is denoted as $V(\lambda)$.
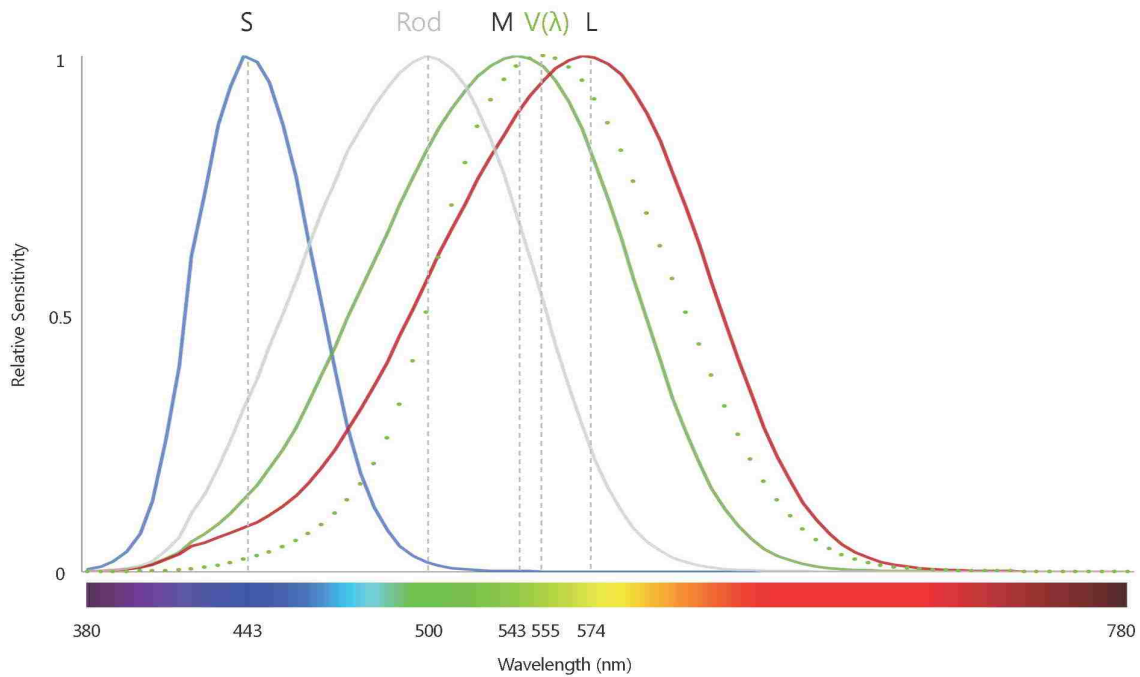
Figure 2.5. Relative spectral sensitivity of S, M, L cones, rods and $V(\lambda)$

The non-visual photoreceptor, ipRGCs, is a recent finding. Before the discovery of ipRGCs, studies on mice showed that mice with retinal degeneration retained circadian photoentrainment ability.[14][17][18][19] Even blind humans showed similar results.[20] This result was explained then, as the work of few surviving rods and cones that albeit insufficient for visual transmission was

sufficient for circadian system. However, when transgenic mice with complete lack of rods and cones showed same result and retained other non-visual light responses such as pupillary reflex, existence of another photoreceptor other than rods and cones was acknowledged.[21][22][23][24] This photoreceptor called ipRGCs was discovered very recently in 2002.[6][7] As the name ipRGCs suggest, these Retinal Ganglion Cells (RGCs) are photosensitive even when isolated from rods and cones due to melanopsin, photopigment in ipRGCs, making it 'intrinsically photosensitive' (ip). When isolated from other photoreceptors, ipRGCs are most sensitive to light in the blue part of the spectrum (around 480nm), is only excited with bright light above the threshold for rod vision and has very slow response (several seconds) to quick changes in light patterns.[6]

The exact relationship between ipRGCs, rods and cones are just beginning to be discovered. ipRGCs perform as a pathway for light information as any other Retinal Ganglion Cells by receiving synaptic inputs from other cells contributing to the visual system in the retina.[25][26][27][28][29] Moreover, a study showed ipRGCs receive photic input from other photoreceptors even when mice ipRGCs were not directly photosensitive due to absence of melanopsin.[30] These melanopsin knockout mice still retained major non-visual responses such as pupillary reflex and circadian photoentrainment albeit with severely lower behavioral and phase resetting response.[30][31][32] Studies also showed that remaining non-visual responses were completely absent in animals lacking rods, cones and melanopsin.[33][34] This shows without rods and cones input to compensate for absence of melanopsin, ipRGCs won't receive any light signals. Likewise, when the whole ipRGCs were knocked out (not only melanopsin gene), circadian photoentrainment capability was completely absent. This resembles results from studies on animals lacking all photoreceptors.[35][36][37] These studies show that ipRGCs are the principle

photoreceptor for circadian system, and rods and cones support non-visual responses by influencing activity of ipRGCs.
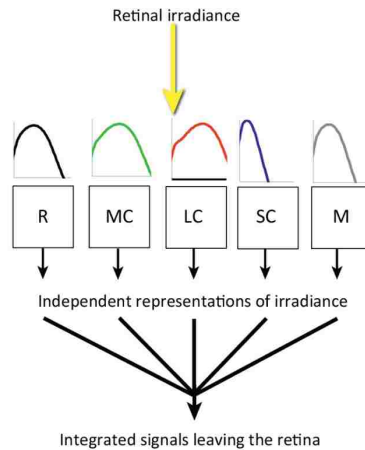
Figure 2.6. Five photoreceptors in non-visual system [38]

Thus, the question remains; when all five photoreceptors may be contributing to non-visual responses, how can spectral sensitivity curve be defined for the non-visual system? Various studies tried to identify contributions of each photoreceptors in visual and circadian response.[39][40][41][42][43][44][45][46] To summarize, melanopsin only functions when light stimulus is bright (when rods are saturated) and in these light levels, cones sends signals during abrupt light changes to ipRGCs while melanopsin registers light signals when light is sustained. Therefore, ipRGCs and non-visual system further down the path can be responsive to much lower levels of light as 1 lux in highly controlled environment to suppress melatonin because of input from rods and cones.[47][48] These contributions from rods and cones are highly dependent on light context as can be seen in switching of photoreceptors managing pupillary light reflexes.[38] For instance, in abrupt increase of irradiance, pupil area decreases from rods and/or cones input. After this

9

constriction, pupil gradually relaxes. When threshold for melanopsin activation is reached, pupil diameter is held constant after around 3 minutes when melanopsin contribution increases over rods and cones.[44][49] In this condition, when light is turned off, pupil constriction persists for few seconds due to melanopsin activation.[50] This complex pupil activity is dependent on light intensity, spectral content, and exposure duration. Other findings from approximately identical experimental conditions showed different cone contributions across brain regions receiving ipRGCs input.[51][52] This suggests that these regulation of altering reliance of rods, cones and melanopsin are not constant.

To further complicate matters, there are at least 5 different types of ipRGCs which may all have different neural processing path (not just to SCN) with different functions within the non-visual system.[53] Rea et al.[54] and Amundatottir et al.[55] tried to address this complication by coming up with a spectral sensitivity curve that could explain combination of these photoreceptor's exchange of light information. Yet, due to the context dependent, unpredictable and complex photoreceptor contribution in non-visual system, it is challenging to represent all non-visual responses in all lighting conditions with one spectral sensitivity curve. Multiple spectral sensitivity curves could be used for different lighting conditions in the future to better represent non-visual spectral sensitivity. Nonetheless, until further research, there are insufficient data to develop these calculation functions.

At present, it is important to recognize that in the early stages of non-visual system light is directed to five photoreceptors, which later combines to an integrated representation of non-visual lighting conditions. Until further research on the integration process, Lucas et al. suggests to record each of these data including photopic illuminance as well as melanopic illuminance.[38] Then, what spectral sensitivity does melanopsin have? Regarding spectral sensitivity curve, there is no consensus on the exact form of this seemingly autonomous photopigment. However, various studies
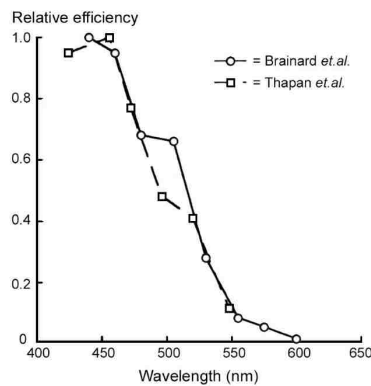
Figure 2.7. Relative spectral sensitivity of non-visual system [5]

(measured using melatonin suppression as marker)

based on responses in humans, non-human primates and rodents show that it peaks at the blue end of the spectrum (447-484nm). [6][24][33][43][44][39][56][57][58] Currently, stemming from various researches, different versions of the curve exists. [38][44][54][56][57][58] Early studies by Brainard et al. and Thapan et al. measured spectral sensitivity of human non-visual system by measuring melatonin suppression levels.[56][57] Curve fitted around these results show peak spectral sensitivity at around 464nm.[56] More recent findings suggest around 480nm.[44][59][60] Various other curves are fitted around these experimental findings, such as curves developed by Gall, Enezi et al. (as adopted by Lucas et al.) and Rea et al.[54][38][56][57] Currently in lighting research for built

11

environments, there are two mainstream curves. First, the melanopic curve developed by Enezi et al. (adopted by Lucas et al.), which only looks at spectral sensitivity of melanopsin in ipRGCs.[11][38] Second, the Rea curve which takes account of impact of rods and cones in circadian entrainment giving the negative value on the curve.[54] Applications of these action spectra in are explained further in section 3.1.1. Metrics.

2.3. Circadian System

Neural signals from ipRGCs are sent to various parts of the brain. These different connections lead to different functions within the non-visual system such as pupillary light reflex, DNA repair and production of other hormones. The path that has been most extensively studied, and perhaps the main function within the non-visual system is the path leading to SCN. This part of the brain is responsible for regulating circadian rhythm of the body. This section explains circadian rhythm is and how it can be entrained.

2.3.1. Circadian Rhythm

Most organisms have behavioral and physiological changes that occur regularly over the 24-hour cycle. This includes behaviors such as sleep-wake cycle and neuroendocrine changes such as core body temperature, blood pressure and adjustments in hormone levels regulating these behaviors. This 24-hour rhythm of living things is called circadian rhythm, with Circa literally translating to 'About' and Dies to 'Day' to mean 'about-a-day rhythm'. This internal rhythm is mostly regulated by the SCN, where signals are sent to paraventricular nucleus (PVN) in the hypothalamus region of the brain. Here, several hormones are regulated including melatonin secretion from pineal gland and cortisol from pituitary gland. Secretion of these hormones are in part or fully regulated by

circadian rhythm. Melatonin is hormone that is secreted in the dark phase of the circadian rhythm sending chemical signals throughout the body to synchronize physiological activities such as promoting sleep, production of other reproductive hormones, activating antioxidant enzymes for antiaging process and interacting with the immune system.[61][62][63][64] High levels of melatonin is secreted during night(dark) and low levels during day (light). When melatonin secretion decreases, cortisol takes over. This hormone is related to activity, helping to release energy needed to transition from sleep-state to activity. Concentration of this hormone peaks around waking time and is lowest at night when melatonin is taking control. Although cortisol is also regulated by circadian rhythm, it is affected by other factors such as stress. These circadian rhythms of physiological processes regulate sleep/wake cycle, maintain health and modulate cognitive function of living organisms. In this study, circadian system will be referring to non-visual system's circadian function.

2.3.2. Circadian Entrainment

Circadian cycle is not exactly 24 hours, ranging between 23.5 and 24.7 hours with 24.2 hours in average.[65][66] This means that over time, human internal circadian rhythms become unsynchronized with the external light/dark cycle. Therefore, the main role of the circadian system is to entrain this internal circadian rhythm to be in sync with the external 24 hour light/ dark time cues. Circadian system reacts to various light exposures (not just daylight). For instance, a study found that people who were only exposed to sunlight and fire light synchronized their circadian rhythm to the solar time. People who were exposed to electrical lighting after sunset had delayed circadian rhythm compared to the previous group.[67] This delay or shifting of

13

circadian rhythm is called phase shifting. Phase shifting can be seen in night shift workers or people who travelled across different time zones. In the case of jetlag, the person is entrained to light/dark cycle of another time zone. Phase shifting occurs as that person's circadian rhythm gets entrained to the current time zone by external time cues.
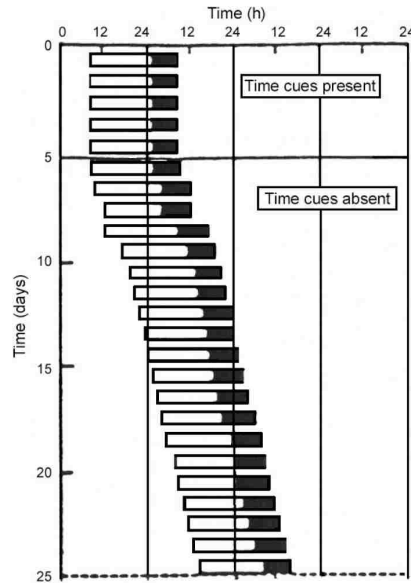
Figure 2.8. Sleep wake cycle of an individual over 25 days [5]

As explained above, stimulation of ipRGCs is dependent on intensity, spectrum and duration of light. In addition, timing, photic history, spatial distribution and age also effects activation of the circadian system. The following sections explains these dependencies in detail.

i. Intensity

Zeitzer et.al measured phase shift of melatonin levels by exposing subjects to cool white (4100°K) fluorescent lamp to study intensity of light required to stimulate circadian system (Fig 2.9). Each subject was exposed to constant illuminance for 6.5 hours.[68]

14
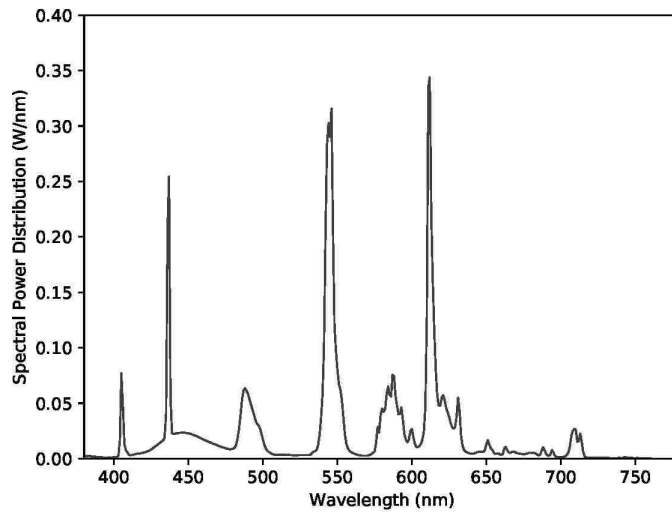
Figure 2.9. 4100°K fluorescent lamp spectral power distribution

This light exposure duration was centered 3.5 hours before subject's minimum core body temperature (usually the highest melatonin concentration) and illuminance at the cornea ranged from 3 to 9100 photopic lux for different subjects. Results showed light exposure of around 120 photopic lux was enough to initiate melatonin suppression and approximately reach 50% of melatonin suppression levels (Fig.2.10). Illuminances above 200 lux saturated melatonin suppression levels and around 550 lux saturated phase shift response. Cajochen et al. studied intensity of light needed for subject alertness in identical test conditions.[69] Results were similar to the study above, with full subject alertness at around 300 photopic lux and around 100 lux to achieve 50% of full alertness under given spectra.

These studies show that ambient light levels in a room (90-500 lux) during early biological night has significant impact in delaying human phase response curve. However, results from these studies

15

should be read with caution as this is the result from controlled laboratory settings. In both studies, subjects were left in dim conditions for several hours before the experiment. This greatly differs from typical lighting conditions in everyday life, leaving questions about what the impact will be in the typical environments. Nonetheless, researches such as these provide guidelines for lighting in the built environments. There are currently no known threshold levels required to support circadian entrainment outside controlled conditions. WELL building standard states 250 Equivalent Melanopic Lux at 75% or more workstations on vertical plane with at least 4 hour exposure.[70] This number is based on informed judgements derived from recent studies.[68][71]
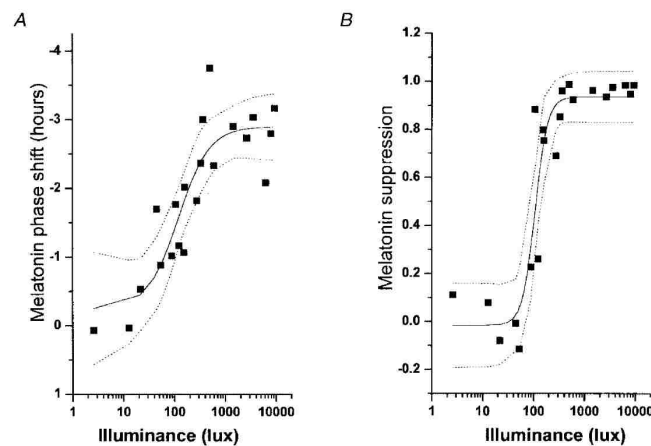
Figure 2.10. Illuminance response curve measured by melatonin phase shift and suppression [68]

ii. Spectrum

Spectral sensitivity of melanopsin peaks in the short wavelength region of visible spectrum. Although exact spectral sensitivity curve for the circadian system is unknown, it can be deduced that blue rich light is more likely to entrain the circadian system. Spectral sensitivity of non-visual system is explained in section 2.2.

16

iii. Duration

In both rodents and humans, short interval of light was needed to suppress or activate secretion of melatonin. In a study on rodents, exposure to short intervals of bright light for less than 1 minute was enough to start suppressing melatonin levels in darkness.[72] Decrease in melatonin levels was measured after 2 minutes. For humans, melatonin levels decreased in less than 10 minutes.[73] When light was extinguished melatonin increased in less than 15 minutes.[74] The reported minutes for these studies are not exact times required for change in melatonin levels as blood was not sampled in shorter intervals than mentioned above.
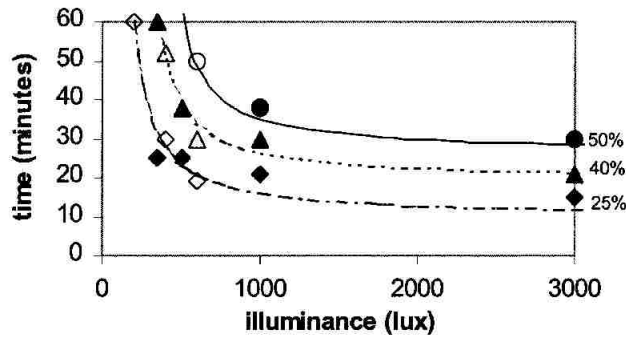
Figure 2.11. Time required to measure melatonin suppression [75]

Circadian phase shift varies exponentially with duration.[17] McIntyre et al. showed that with 1000 lux illuminance at the cornea, it takes around 20 minutes for 25% melatonin suppression, while 500 lux requires 1 hour.[74][76] This study shows that higher intensity requires shorter duration of light exposure for same melatonin suppression effect. A study by Chang et al. exposed subjects with much brighter light of 10,000 lux.[71] Comparing melatonin suppression for different durations of 0.2 h, 1 h, 2.5 h and 4.0 h showed shorter hours were more efficient in suppression of melatonin and circadian phase shifting when tested with bright light.

17

iv. Timing

Timing affects circadian phase shift. If the exposure time follows the solar time, circadian rhythm will sync with the natural night/day cycle. However, exposure to light at night (LAN) delays circadian rhythm. In contrast, exposure to light in early morning advances circadian rhythm.

v. Photic History

Studies have shown sensitivity of ipRGCs to light exposure varies with prior photic history. [77][78][79][80][81] Measured melatonin suppression levels showed sensitivity to light decreases over time with exposure and rises with absence of light. For example, a study compared melatonin suppression levels for two groups with different photic history (1 week of varying prior exposure).[7] When exposed to 3 hours of light (500 lux), group with prior exposure to bright daytime light (5000-7000 lx) had less melatonin suppression compared to group with dim light (<200 lx) photic history. Another study showed prior photic history as little as 3 days changed magnitude of melatonin suppression.[79] Photic history also had effect in changing amplitude of circadian phase shift response for subject with low light exposure history.[81]

vi. Spatial Distribution

Two studies showed that light exposure to the lower part of the retina showed greater suppression.[8][9] However, ipRGC's dendrites are spread throughout the retina making the whole area photosensitive. More researches are needed to confirm sensitivity of spatial distribution in the retina for circadian system.

18

vii. Age

Age also influences circadian entrainment. As people age, their lens yellows and darkens, reducing transmittance of blue spectra of light. This reduces amount of blue light stimulating ipRGCs and thus identical light is registered differently for individuals depending on their age.
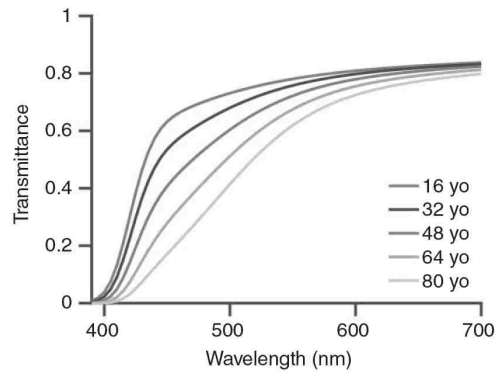
Figure 2.12. Yellowing of lens depending on age [90]

These dependencies (intensity, spectrum, duration, timing, photic history, spatial distribution and age) affect how ipRGCs registers light, and consequent physiological response. It is therefore important to understand how these factors vary within built and natural environments.

3. Current Status of Applications of Circadian Rhythms in Built Environments

Chapter 2 reviewed the current research on circadian rhythms in photobiology, chapter 3 focuses on the research in building sciences. It can be argued that the most important and long-term effect of exposure to daylight for the non-visual system is synchronizing our circadian body clock to the local time.[16] However, people in the US are spending around 90% of their times indoors and in some cases in biological darkness.[82] It is therefore critical to understand the lighting conditions in built environments and its impact on circadian rhythms. Research on applications of circadian rhythms in building sciences is quickly advancing and can be grouped into two: simulation and physical measurements.

3.1. Simulation

3.1.1. Metrics

Photopic illuminance or luminance is calculated by weighting spectral power distribution curve of incident light with $V(\lambda)$. (Fig. 3.1.) To calculate the circadian specific illuminance or luminance, a similar method can be utilized with a circadian curve $C(\lambda)$. $C(\lambda)$ has different spectral sensitivity to the photopic curve $V(\lambda)$ with peak sensitivity in the blue region (480nm). Therefore, photometric units weighed with $V(\lambda)$ such as photopic illuminance(lx) and photopic luminance(cd/m2) are not applicable to quantify the amount of light stimulating the circadian system. Currently, there are no consensus on the metrics to represent circadian lighting in the

20

literature. Varying metrics and units are used in different studies to quantify circadian lighting. The following sections describe different metrics found in literature.

a)
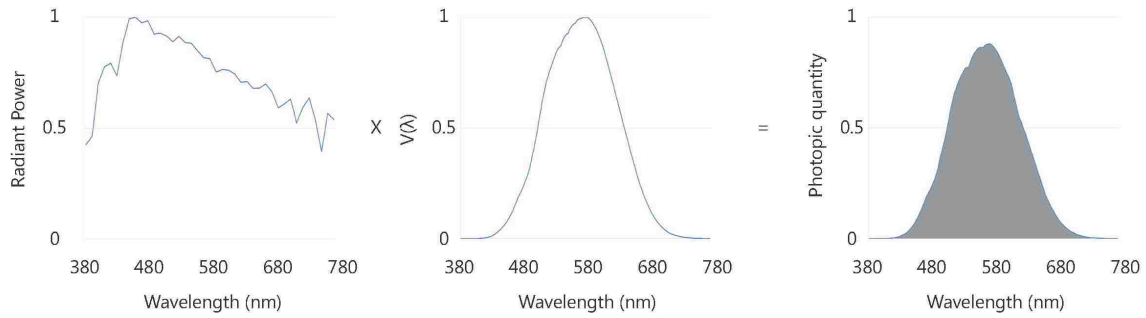
b)
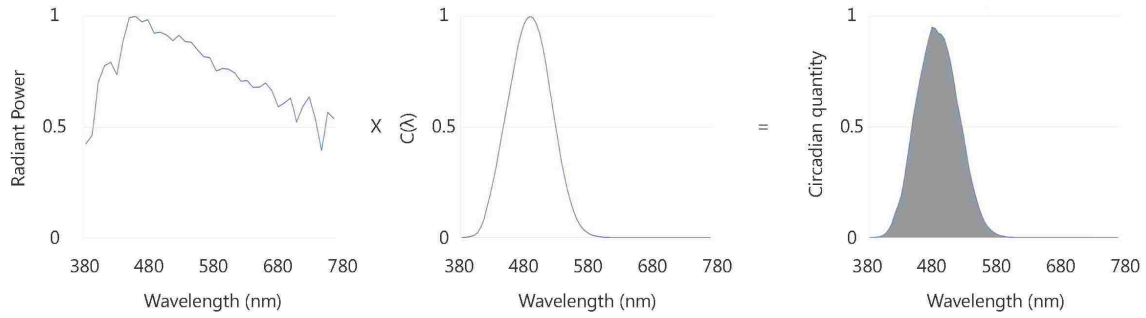
Figure 3.1. Luminance calculation: a) photopic calculation b) circadian calculation

i. Equivalent Circadian illuminance

Pechacek et al. used metric called circadian efficacy W-C(λ) to quantify circadian weighted value in Watts, where absolute radiometric spectrum(W) is weighed with C(λ) to show circadian potential.[83] This metric was designed to compare circadian efficacy for different light sources by finding out the photopic illuminance(lx) needed to induce the same W-C(λ) as the reference light

source. Outcomes from Cajochen et al. was used to define intensity threshold values for the reference light source.[69] This research demonstrated that subjects in a room lit with 4100°K Philips fluorescent lamp (surface material properties are not reported, it is assumed to have white walls) reached full circadian stimulus with 300 photopic lux at the cornea after 6.5 hours. This photopic illuminance translates to 0.27 W-C(λ).[83] The value of 0.27 W-C(λ) may change with different C(λ) functions. The author used an experimental C(λ) developed by Philips Lighting, based on data from Brainard et al. and Thapan et.al.[56][57] Other light sources will require different photopic illuminances to arrive at 0.27 W-C(λ). For instance, requiring 210, 190 and 180 lux for D55, D65 and D75 respectively. The concept of deriving photopic illuminances required by different light sources to have same circadian efficacy as the reference light source is called equivalent circadian illuminance.

This metric is also utilized by Anderson et al. in assessing circadian potential of a space.[84] The study references additional research from Phipps-Nelson et al. to define the reference light for full circadian stimulus; Thorn 2L (36W) fluorescent lamp 1056 lx.[85] This reference light is approximated with F7 illuminant in the study. A linear ramp function is introduced to set a lower and upper bound for the likelihood of circadian stimulus, with equivalent circadian illuminance from 4100°K Philips fluorescent lamp and F7 as lower and upper bound respectively.

Equivalent circadian illuminance for F7 reference light is provided as 960, 870 and 830 lx for D55, D65 and D75 respectively. In subsequent study, D55 is used as a reference light to compare range of different illuminants and set a guideline with applied linear-ramp function.[86] This metric does not provide absolute values, but relative values for comparing one source of light against a

22

reference light source. This is useful in comparing circadian effectiveness of different light sources that may produce same visual effect. Nonetheless, the equivalent circadian illuminance values need to be recalculated when reference light is changed, making it inconvenient to set a solid guideline.

ii. Absolute Circadian lux

For consistency in calculating illuminance of $C(\lambda)$, it should follow conventional calculation method used in photometry; taking the luminous efficacy coefficient (area under the curve) by normalizing $C(\lambda)$ peak (480nm) from 1 to 4557 lm/W.[11] This high value is obtained when $C(\lambda)$ developed by Enezi et al. is normalized to 683 lm/W at 555nm. This approach is consistent in calculating both photopic and scotopic illuminance. However, the resultant values are extremely high due to its scaling. This will inevitably result in confusion in application.
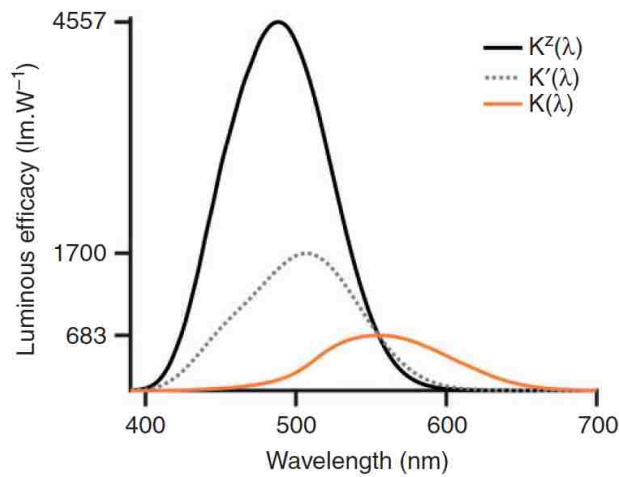
Figure 3.2. Photopic, scotopic and melanopic luminous efficacy function [87]
All function normalized to 683 lm/W at 555nm

iii. Circadian lux

Inanici et al. used metric called circadian lux, where spectral distribution of a light source is weighed with $C(\lambda)$ and it's luminous efficacy coefficient.[88] This method is similar to getting photopic illuminance(lx) by multiplying absolute radiometric spectrum with $V(\lambda)$ and its luminous efficacy coefficient of 179. This particular number is derived by scaling $V(\lambda)$ from 1 to 683 lm/W (luminous efficacy at max peak of 555nm) and calculating the area under the scaled curve. The author calculates luminous efficacy coefficient for $C(\lambda)$ by normalizing its peak (460 and 480nm for Rea et al. and Lucas et al. curve respectively) to 683 lm/W.[54][38] Scaling $C(\lambda)$ to match $V(\lambda)$'s maximum height at 555nm (luminous efficacy of 683 lm/W) is a method suggested by Rea et al.[89] The resulting luminous efficacy coefficient for $V(\lambda)$ is 130 and 148 for Rea et al. and Lucas et al. function respectively. Calculating circadian lux from this method, 4100°K Philips fluorescent lamp with 300 photopic lux is equivalent to 122 and 80 circadian lux (for Rea et al. and Lucas et al. curves, respectively). This metric gives absolute values in circadian lux that can be used like photopic lux to calculate how much light is being received to stimulate circadian system.
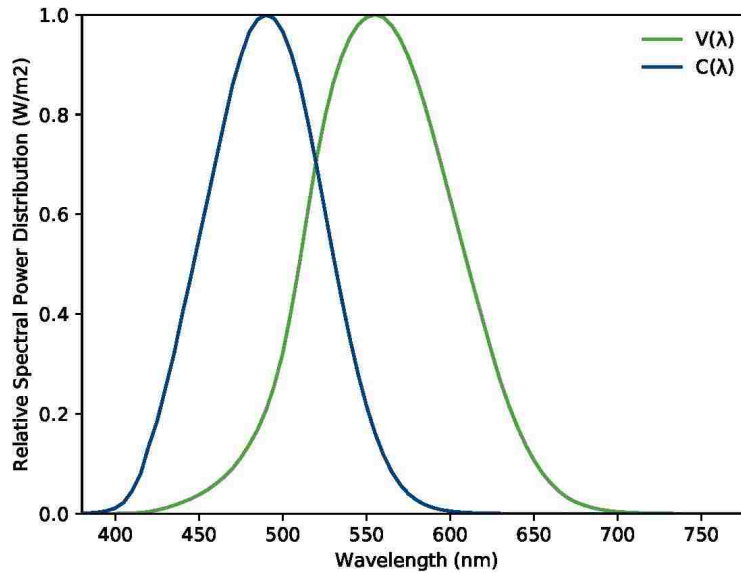
Figure 3.3. Photopic and melanopic curve scaled to have equal peak luminous efficacy

24

iv. Equivalent Melanopic lux

Most recent metric scales $C(\lambda)$ to have the same area under the curve as $V(\lambda)$ to give values in equivalent melanopic lux (EML).[38] The term melanopic is used to reference $C(\lambda)$ curve that is entirely weighted by the sensitivity of melanopsin within ipRGCs. This method of scaling $C(\lambda)$ ensures that equivalent melanopic illuminance is identical to photopic illuminance for a theoretical equal energy light source. In other words, this metric scales the $C(\lambda)$ so that the area under $C(\lambda)$ matches the area under $V(\lambda)$. Therefore, the conversion between Circadian lux and
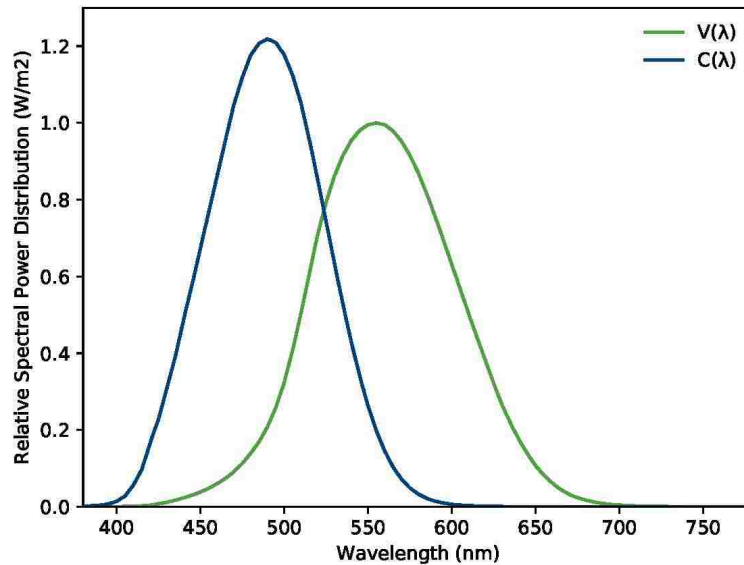
Figure 3.4. Photopic and melanopic curve scaled to have equal integrated area

EML is a linear conversion. The scaling in photopic and EML calculation is 179 (photopic is scaled to match 683 lm/W at 555 and EML is scaled to match the area under the photopic curve); and the scaling in Circadian lux (when scaled to match 683 lm/W at its peak) is 148. Conversion factor from Circadian Lux to Equivalent Melanopic Lux is (179/148 = 1.2). Building certification system called WELL building standard uses this metric to require 250 EML at 75% or more

25

workstations on vertical plane with at least 4 hour exposure.[70] 250 EML is equal to 226 photopic lux from D65, and is based on informed judgements derived from recent studies.[68][71] Konis also uses this metric by converting annual simulation result of photopic illuminance(lx) to EML.[66] Conversion factors for each hour is calculated based on relative direct and diffuse illuminance from the climate file. Direct and diffuse illuminance is assumed to correspond to D65 and D55 respectively, with D65 having conversion factor of 1.1 and 1.0 for D55. This conversion factor is then applied to hourly photopic lux results to convert to EML. The study references 250 EML used in WELL building standard to set a minimum stimulus requirement. Amundadottir et al. also basis EML to define a unitless factor called relative spectral effectiveness (RSE).[90] RSE can be used to show the relative relationship between spectrally-weighted quantities and non-weighed (both radiometric and photometric) quantities. Values of RSE can further be used to calculate absolute values of irradiance or illuminance, as well as equivalent circadian illuminance. Based on its simplicity to compare photopic and circadian values, EML is adopted as the unit to report circadian lux and illuminance in this study.

iv. Circadian Stimulus(CS)

A different metric called circadian stimulus (CS) is used by Rea et al.[91] This metric uses $C(\lambda)$ curve that is developed by Rea et al., weighted by the sensitivity of melanopsin photoreceptor (ipRGC), 3 cones and rod. Calculating illuminance from this $C(\lambda)$ gives values in circadian light (CL). Normalizing CL with a scalar factor to match the photopic illuminance of CIE illuminant A with 1000lx gives CL_A. CL_A is defined as "irradiance at the cornea weighted to reflect the spectral sensitivity of the human circadian system as measured by acute melatonin suppression

after a one-hour exposure".[92] Figueiro et al. defines threshold of CS of 0.3 or greater for at least

1 hour in early morning. This is equivalent to 180 lux with D65.
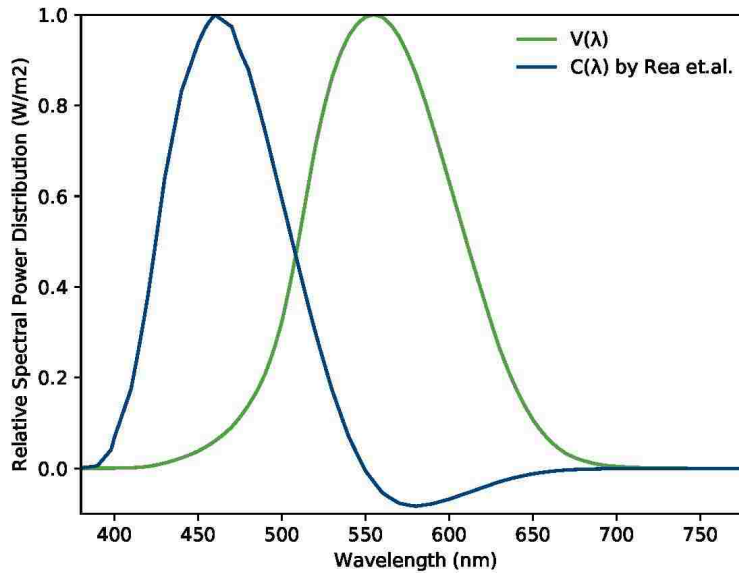
Figure 3.5. Photopic curve and circadian curve developed by Rea et al.[91]

Applying different methods of normalization for calculating the circadian lighting values, as well

as different methods of quantifying the amount of light stimulating circadian system created

variety of metrics. Moreover, different versions of C(λ) outputs diverse simulation results that can

be confusing when comparing results from various literature. Until a unified metric for circadian

light is developed, readers should take caution in understanding the results in literature.

3.1.2. Simulation Period

Sensitivity of circadian system is influenced by both short term (hours) and long term (days and weeks) optical radiation. Short term exposure during the course of a day helps to regulate human circadian rhythms. Short term exposure (i.e. few hours during the daylit hours) helps define sensitivity of light exposure, with higher exposure during the day resulting in lower sensitivity during the night. Continued exposure to similar short term radiation characterizes long term exposure, called photic history. Photic history (from few days to few weeks prior light exposure) also influences sensitivity to light during the night. For example, research shows low intensity photic history amplifies sensitivity to light exposure by 60-70%.[81] Therefore, it is important to study both long term and short term exposure in simulation to fully understand circadian stimulus in a space. Research in circadian simulation can be separated into two methods; point-in-time and annual simulation.

Pechacek et al.[83] utilized Daysim[93] to map Daylight Autonomy(DA)[94] of circadian light on a vertical analysis grid. This cumulative annual data was applied to study a hospital patient room design and the impact of architectural decisions. Cumulative annual simulation period may be useful in reviewing overall architectural orientation, but is limited in closely studying circadian potential of timing and duration of light in a space. Andersen et al. and Mardaljevic et al. also uses Daysim to get cumulative annual data from temporal maps.[84][86] The studies simulate 4 opposing orientations on each vertical nodes. Resulting temporal maps are further divided to study the timing of exposure. Daylit hours are divided to 3: early to mid-morning (6am -10am), mid-morning to early evening (10am – 6pm) and night time (6pm – 6am). From this division, the authors developed a new graphics representation called 'sombrero plot' for circadian potential of

28

view direction and timing of each node. Although this study is still only looking at cumulative annual data, its differentiation in light exposure times and directions helps to study circadian potential of a space in more detail. However, even with additional information of timing, the studies only show the arithmetic mean of all annual hourly illuminance values between binned hours. For example, result of 40% could both mean 40% of circadian potential for 100% of the year, or 100% circadian potential for 40% of the year, or somewhere in-between these two extremes.

Amundadottir et al. also used Daysim to simulate annual circadian response.[87] The results were shown in both temporal maps and in grid format. The temporal map plots % frequency of average hourly circadian response reaching threshold value. These temporal maps make it easier to compare effectiveness of different views, occupancy schedules or space types. Shorter time periods can also be studied in grid format where each node is presented with octagon shape to represent view direction. These octagons are colored according to percentage of frequency that view direction reaches above the threshold value. Shorter time period graphics can be used to compare circadian stimulus for summer (May-August) and winter (Nov-Feb) periods, as well as two different schedules (and corresponding space occupation times) over the course of a day. This type of post processing the result is useful in understanding short term exposures.

Konis further post processes annual simulation result to show both short term and long term exposures.[66] The author sets daily minimum threshold value as 250 EML in-between 7-10 am. Varied results from daily to weekly or monthly to yearly exposures can be viewed. Daily circadian effective stimulus is shown in vector grid view, where represented vectors indicate which view direction met the minimum threshold. For yearly result, polar plot is used to indicate whether at

least one vector from a node met the threshold value. The author developed "stimulus frequency" indicator that grades a node vector from A to F depending on the percentage of a week that meets daily minimum threshold. This can be visualized with Circadian Effective Area (CEA) that looks at % of analysis area that at least one vector meets minimum threshold from stimulus frequency indicator. It can further be processed to take monthly mean of CEA to plot on a grid to visually represent spatial variations over monthly period. Vector information can be layered on to show the percentage of hours meeting the daily minimum in a month for selected view direction. Various ways of representing simulated data such as these can help designers to visualize the daily, monthly and seasonal variations of circadian stimulus in a space.

Point in time simulation approach was used by Inanici et al.[88] Instead of using Daysim to get numerical results, the authors used Radiance[95] to visualize a space at a specific point in time. From these visualizations, illuminance values at the eye were taken over a time step period throughout a day to show variations in circadian stimulus. Time step visualization simulation method gives flexibility in the choice of view directions as well as ability to use measured sky data. To understand seasonal variations, additional days will need to be simulated throughout the year.

3.1.3. Spectra

Circadian entrainment is dependent on various factors: intensity, spectrum, duration, timing, spatial distribution, photic history and age. The spectra of light is especially important, with blue rich light having more potential to stimulate circadian system. Nonetheless, it is not only the spectra of the light source that effects human circadian entrainment. As light is reflected multiple times in a space, spectral transmission and reflection properties of interior surfaces along with the

30

spectral properties of the light source determine the resultant light spectra entering the human optical system. In current literature this is not well addressed, with various studies assuming a space to be spectrally neutral (in shades of grey and white).[83][84][86][66][87][96]

Inanici et al. modelled both the light source and the surface material with spectral properties to study circadian impact in a space.[88] Using the Radiance gensky command, point in time colored skies were modelled to match the overall sky luminance and the estimated or measured Correlated Color Temperature (CCT) values. Point in time sky data were used to visually simulate different views in a spectrally rendered space. For increased spectral accuracy, the study implemented technique developed by Ruppertsberg and Bloj with 9 channel bins instead of typical 3 bins (RGB) used in Radiance.[97][98] From these renderings, luminance distribution and illuminance values could be studied. Hourly results in April showed that occupants looking directly at the window received more circadian lux than individuals facing the wall. The simulated room was also colored with contrasting colors (Macbeth color #3, blue and Macbeth Color #15, red) to clearly demonstrate the effect of colors in circadian entrainment. The white or blue walls provide higher circadian lux values in comparison to the red one. This was most evident in June simulation, where spectra of the sky is blue rich (25000°K). Spectrally accurate visualizations can help design professionals to visually assess the effect of material color on circadian response. This will be especially useful when a space has complex layout. However, multi-channel simulation method requires physically accurate material library, which can be difficult to obtain.

31

3.1.4. Additional Performance Criteria

Variable criteria such as view, duration, timing and photic history have been addressed in literature review in Chapter 2, but this is harder to address in a simulation. This section explains how some of these variables are incorporated in literature.

i. Timing, Duration and Photic history

Circadian sensitivity to light exposure changes depending on the timing, duration and photic history. These criteria are often influenced by the built environment with most people spending their daylit hours indoors. Andersen et al. and Mardaljevic et al. studied timing of exposure through cumulative annual simulation as discussed in 3.1.2.[84][86] Although the study divided the hours into 3 parts (early to mid-morning, mid-morning to early evening, and night-time), it did not address the impact of the duration of light or the photic history. Amundadottir et al. developed a unified model to include all factors effecting circadian entrainment by simplifying assumptions from photobiology studies.[55] This methodology was later applied in a health care case study building.[87] In the study, building schedule is used to simulate varying light exposures dependent on timing and duration. Konis examines the duration of light exposure through calculation of stimulus frequency.[66] The author sets a threshold of 71% stimulus frequency, requiring at least 5 days of exposure meeting the threshold value of 250 EML in the early morning. These models of guidelines and calculations in literature are largely based on current findings in photobiology, as well as underlying assumptions made by the authors. Establishing circadian guidelines in the built environment will require more studies from photobiology and substantial number of occupant feedbacks for field-based validation.

ii. View points

Difficulties in assessing light exposure arise due to the dynamic nature of the viewpoints occupants experience throughout the day. Although a probable view direction may be assumed in an office setting, it is not realistic as saccadic eye movements happen in a fixed position and occupants move around throughout the day. Therefore, finding the right view to simulate for the circadian light exposure can be difficult. Andersen et al. simulates for 4 opposing views to show which view direction has the most circadian potential.[84] These views are fixed and covers 180° for each view. Amundattotir et al. simulates each node with 8 view directions on each node.[87] Moreover, varying light patterns are generated depending on 4 evaluation methods. 'Zone-based, fixed' method simulates with fixed nodes and view directions. Random node selection (n=100) and view direction to account for occupant's movements is 'zone-based, random' method. Rearranging these methods to align with the activity schedule is 'activity-based' method. The study reports random light patterns gives more stimulus frequency than fixed method. Moreover, occupant schedule determines the timing of view direction, giving better stimulus frequency when exposed earlier. This method however, assumes that occupant view direction is completely random. In reality, views are more dependent on the furniture layout and varies according to the primary view direction. Konis also simulated with 8 view directions for each node to identify circadian disruptive building zones.[66] The vectors representing views are visually shown when circadian stimulus meets the threshold for the time duration (7-10 am in the study). These views can also show the percentage of stimulation frequency (5 days out of a week) in a year, to identify which node is not receiving enough circadian frequency in a long term. In the case of fixed view situation, only vectors for selected view can be represented. This simulation method can be used to visually identify which fixed view direction is most effective for any area of the space.

3.2. Physical Measurement

The simulation method calculates the circadian response to optical irradiation with assumptions on physical properties of space geometry, material and lighting properties along with basic occupant location and viewpoint. Human beings navigate indoor and outdoor environments in dynamic manner throughout the day. To study the human circadian experience in varying environments, physical measurements are needed. This section reviews previous studies that focus on the physical measurements of circadian lighting conditions.

3.2.1. Specific Measurement Devices and their Calibration Process

Most of the literature uses specially developed devices to capture circadian light exposure. Bierman et al. developed a wearable device called Daysimeter to analyze occupant's light exposure over the course of a day.[99] Two cosine calibrated photosensors placed near the cornea are fitted with custom glass filter to closely match $V(\lambda)$ and $C(\lambda)$ developed by Rea et al.[91] The study does not mention the calibration process for the photosensors, but states that there is less than 2% mismatch error for photopic photosensor. Unlike the sub-additive function $C(\lambda)$ developed by Rea et al, circadian photosensor in the Daysimeter shows additive response. These limitations are addressed by post processing the collected data. It also tracks light levels approaching 100,000 lux, well beyond the human circadian saturation level. Circadian irradiance defined by Figueiro et al. (CL_A) is calculated from the collected data by approximating the data from two photosensors to derive inputs for four spectral sensitivity functions.[92] For most standard illuminants, errors from this estimation were less than 10%. Saturation of circadian system was accounted by calculating circadian stimulus (CS) from CL_A. In a later model of the device, dimesimeter, data is collected

across 3 channels; red(R), green(G), blue(B).[100] These channels were then tested for spatial and absolute response with varying angles and intensity. To calibrate RGB channels to match $V(\lambda)$, photopic illuminance measurements of 750W tungsten-halogen lamp at 2856K were taken with Dimesimeter and calibrated illuminance meter to calculate the calibration constant. Expected errors were mostly less than 5% for standard illuminants. Similar method is utilized for calibrating RGB to match $C(\lambda)$ developed by Rea et al.[91] This method calibrates RGB color space in the equipment to match CIE photopic curve (CIE Y).

Borsuit et al. developed a Camera-Like Light Sensor (CLLS) to measure point in time circadian light levels.[101] CLLS's spectral sensitivity has been previously calibrated to match $V(\lambda)$ and is corrected for vignetting effects.[102] It also takes High Dynamic Range (HDR) photographs quicker than conventional charge coupled device (CCD) camera to capture photopic luminance under highly dynamic lighting conditions. To correct spectral sensitivity to match $C(\lambda)$ developed by Gall, both intensity and spectrum was calibrated.[58] For intensity calibration, different intensities of 470nm monochromatic light was captured by the CLLS and calibrated spectrophotometer to match the correlation of the two circadian weighted radiance (L_{ec})data. Luminance values were calibrated by taking 83 measurements varying from 0.04 to 23871 cd/m^2 with CLLS and luminance meter. Additionally, varying spectra of light from 380 to 780nm in 5nm increments at constant intensity were measured. The raw spectral sensitivity of CLLS was corrected to match $C(\lambda)$ with customized filters. Standard error between $C(\lambda)$ and corrected CLLS sensitivity response was 10.4% when calculated with CIE standard error (F').[103]

3.2.2. Captured duration

Duration of physical measurement of circadian light are categorized into two approaches; capture the light in a point-in-time manner, or to measure the accumulated light data. As circadian stimulus is not instantaneous, Bierman et al. measured the circadian light levels for the duration of a day.[99] The Daysimeter collects activity, temperature and radiation data every second and averages it in 30 second intervals. It can continuously measure the data for 30 continuous days.[104] To analyze the difference in circadian rhythm for night and day shift nurses, the data was analyzed for both 24 hour period, and for 7 day period. 7 day period analysis showed better representation of disrupted consistency and activity patterns experienced by night shift nurses. The point in time approach by Borsuit et al. was used to compare varying patterns of light exposure for different louver types and times.[101] To study full circadian light exposure, point in time method requires time step measurements for varying days.

4. Research Methodology for Capturing Circadian Light

Research in non-visual light is quickly evolving and there is a need to gather more information to understand variability and quantity of non-visual light within the built and natural environments. With more understanding of non-visual light within the built environments, better metrics will be developed to analyze non-visual light in the future. Non-visual light data can be gathered with both simulation and physical measurement. Simulation is a great method when developing a design, but can be costly for existing conditions. To analyze the current condition of non-visual light within the built environments, physical measurements are more convenient and cost-effective. Current method of measuring circadian light requires a special device that are inaccessible and expensive. To address this need, a new method of measuring non-visual light using High Dynamic Range (HDR) photography is developed. Chapter 4 discusses method of measuring non-visual light through HDR photography. It will focus on the details of capturing process, calibration and calculation of non-visual light.

4.1. Capturing Process

It is already established that HDR photography can be used to capture high resolution luminance data of photopic light. These images are post processed and calibrated with physical measurement taken with a luminance or illuminance meter and can be used to analyze visual perception and comfort within the built environments.[105] The capturing process for measuring non-visual light is almost identical to the existing method.

For this research, Canon EOS 5D camera is used to take low dynamic range (LDR) photographs. This camera model has a full-frame sensor (36 mm x 24 mm) which will capture the whole image from a circular fisheye lens without cropping. Using other cameras with full frame sensors would be equally applicable. Sigma 8mm F3.5 EX DG fish eye lens is used which has 180° angle of view. Angle of projection for this lens is mentioned as equisolid from the manufacturer. Equisolid projection compresses objects in the periphery. Equidistant projection maintains angular distances. Actual projection measurement shows the lens in between equisolid and equidistant projection. The projection aberration can be corrected as given in Jakubiec et. al.[106]
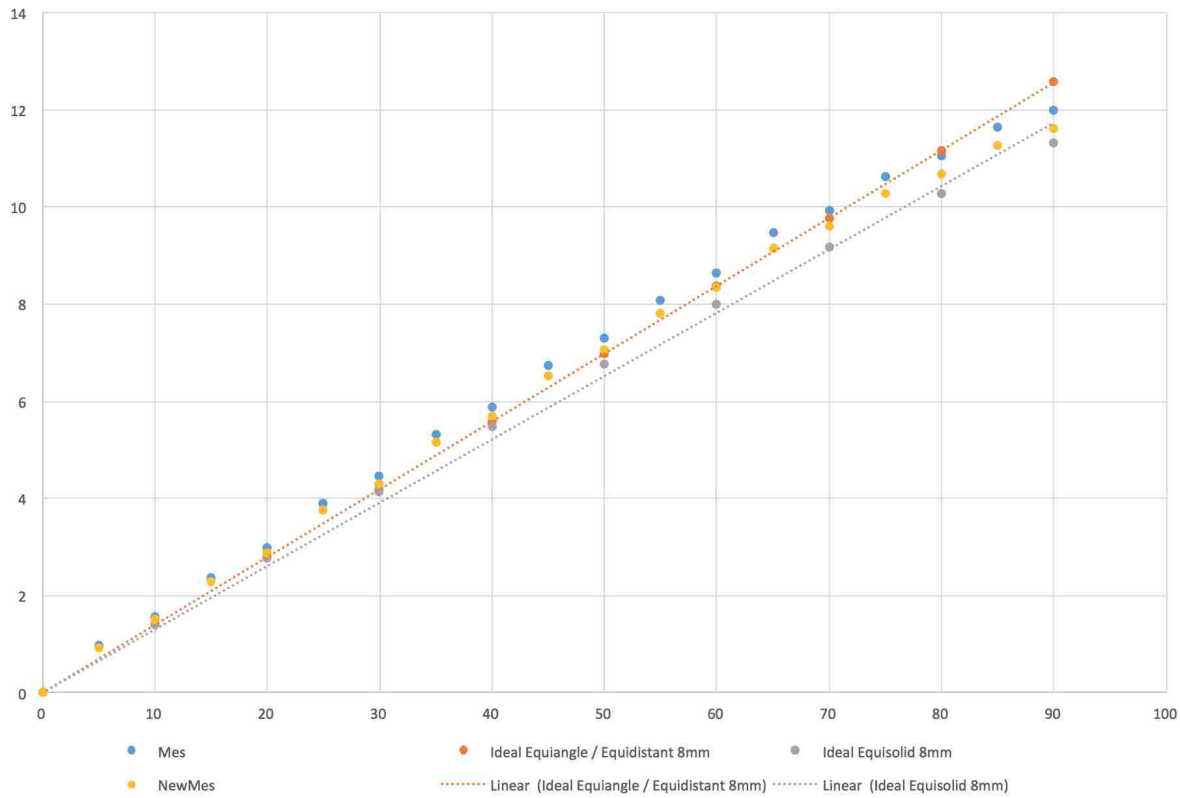
Figure 4.1. Sigma 8mm F3.5 EX DG lens projection angle [107]

Image capture process follows the best practices as specified by Jakubiec et.al.[106][108] Camera aperture is fixed to f11 to retain focus and depth of field of the images. White balance is also fixed

to the daylight setting to prevent chromatic shift between multiple exposures. ISO sensor sensitivity is set to 100. Focus is set to manual to avoid different depths of field. Other features such as image sharpening, noise reduction, auto-bracketing, saturation control and image adjustment is turned off. Lastly, camera is mounted on a fixed tripod to minimize movement between each image. With this set up, multiple LDR photos were taken with varying exposures to capture full variability of light within a scene. Exposures are taken from 30 s to 1/8000 s at 3 stop shutter speed intervals.

These photos need to be calibrated after being assembled into a HDR photograph. For reference physical measurements, a neutral grey card is placed in the field of view as a target to measure luminance. Before and after each HDR capturing process, luminance measurements are taken using Konica Minolta LS-110 luminance meter along with vertical illuminance, Correlated Color Temperature (CCT), CIE XYZ and CIE xy measurements taken in front of the lens using Konica Minolta CL-200A illuminance color meter. As this illuminance color meter calculates CCT with Japanese Industrial Standard (JIS) method, CCT values were recalculated with CIE XYZ values using McCamy method.[109] Explanation about CIE XYZ and different color spaces is provided in section 4.2.4.

Between changing exposures for a HDR photograph, light levels can change. More than 10% difference between pre and post illuminance and luminance measurements denoted instability of lighting conditions during exposures collection of HDR photograph. These HDR photos were exempt from the calibration data. Multiple exposure photographs are processed into a HDR photograph using a software called Photosphere.[110]

4.2. Calibration

4.2.1. Camera Response curve

Initial process of generating a HDR photograph is calibrating the camera response curve. Camera response curve represents how camera RGB sensors capture the real scene luminance. Due to image forming process such as gamma correction, analogue to digital conversion, image digitizer, and tone mappings, RGB values in the captured image has non-linear relationship with the reality. This relationship is computed into a polynomial function using a technique called radiometric self-calibration.[111] Photosphere utilizes this technique when generating the camera response curve for a specific camera. To generate accurate response curve, a daylit scene with large luminance variability is selected. The response curve used in this study is generated from 11 exposure sequences and is shown in figure 4.2.
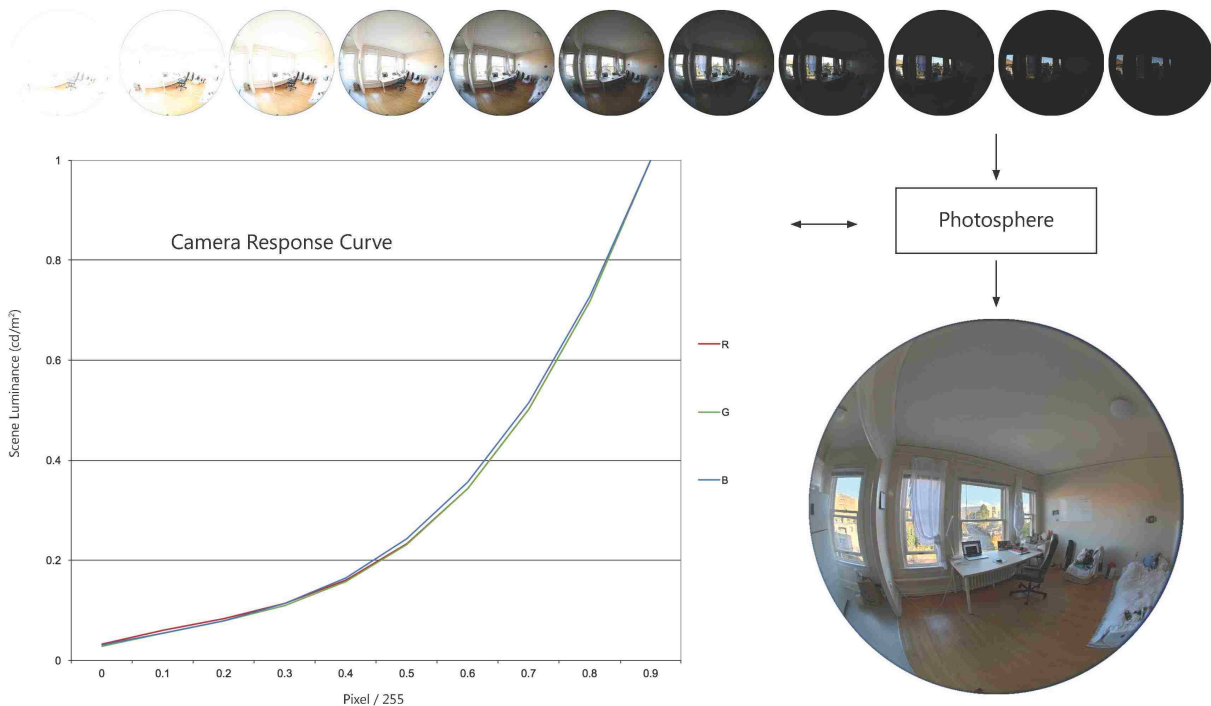
$$R = 1.700195\ x^3 - 1.207507\ x^2 + 0.5161\ x - 0.008788032$$

$$G = 1.674549\ x^3 - 1.166634\ x^2 + 0.5051514\ x - 0.01306627$$

$$B = 1.473927\ x^3 - 0.8755626\ x^2 + 0.4046178\ x - 0.002981866$$

Figure 4.2. Camera response curve for canon 5D determined by Photosphere

These camera response curves vary with different camera models. However, only input for calculation of camera response curve is multiple exposure images. When camera response curve is derived, individual LDR photographs can be accumulated into a HDR image. In the process of generating HDR image, relationship between pixel and scene luminance is corrected as '1 to 1' using the camera response curve. This final HDR image contains pixel luminance data that can extend over the human visual system span (10^{-6} to 10^{8} cd/m^2) due to mathematical affordance of 32 bit.

4.2.2. Post Processing

The raw HDR photograph needs to be post processed to correct aberrations. The process is performed as follows;

i. Crop

HDR image is cropped to cut out unnecessary information outside the captured image.

ii. Resize

Size of the HDR image is scaled to 800 x 800 pixels for efficient image operations. This is an optional step.

iii. Exposure Correction

Exposure of the image is set to 1 for post calculation process.

iv. Vignetting Correction

Sigma 8mm F3.5 EX DG lens shows light fall off (vignetting) for pixels near the periphery of the lens due to its physical structure. Vignetting needs to be adjusted to get the correct luminance values from each pixel. Degree of light fall off for Sigma 8mm F3.5 EX DG lens was calculated to apply a digital filter to HDR photographs. To develop a digital filter, camera setting was fixed to same as setting for taking HDR photographs. In the middle of field of view, was a grey card target to measure luminance. It was then rotated 90° in increments of 5°, taking HDR photographs and luminance measurement from the target with each rotation. Luminance of the target was later compared with HDR photographs and physical measurement for each rotation to assess degree of luminance loss.

42
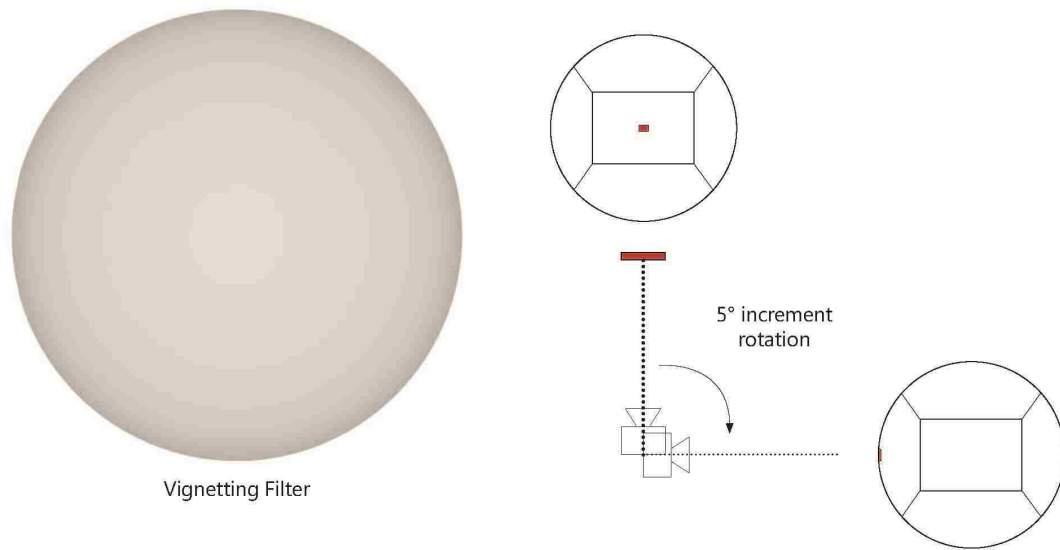
Figure 4.3. Vignetting mask for Sigma 8mm F3.5 EX DG lens at f11

v. Cosine Correction

Sensors for illuminance color meter capture the incident light in hemispherical projection. As Sigma 8mm F3.5 EX DG lens captures light in between equidistant and equisolid projection, the combined HDR photographs needs to be adjusted to match cosine projection. Process for cosine correction from an equidistant projection is computed through HDRscope.[112] The process calls Radiance pinterp command to transform equidistant projection to hemispherical (cosine corrected) projection.

pinterp –vf input.hdr –vth –x resolution –y resolution –ff input.hdr output.hdr

Figure 4.4. Cosine corrected image

vi. Illuminance Calibration

Cosine corrected HDR photographs can be calibrated with illuminance measurements. Illuminance calibration is preferred in this study, as not only illuminance (CIE Y), but entire suite of CIE XYZ values are utilized for color calibration (further explanation for calibration is in the next section, 4.2.3.). Photopic illuminance calibration assures that the total light energy is accounted for in the calculation process to assure accuracy in circadian illuminance output, even in the absence of overflow correction.[106] For photopic and circadian pixel scale luminance accuracy, overflow correction is recommended as described by Jakubiec et.al.[106][108]

4.2.3. Color Calibration

The reason for further calibration with CIE XYZ is to check ability of the camera sensors to accurately capture spectral properties of incident light. Having different spectral sensitivity than $V(\lambda)$, circadian measurement is highly sensitive to blue spectra of light. Although photopic measurement from $V(\lambda)$ is also color dependent, these measurements are calibrated with devices that measure photopic light units. As mentioned in chapter 3.2., there are very few devices that can measure circadian light and these devices does not give EML as circadian light unit. Thus, to calculate circadian light through HDR photographs, camera sensors need to be tested for their accuracy to capture correct color of light. Then, what device can be used to test color accuracy of camera sensors to capture circadian light? One option to study color accuracy of camera is to use spectrophotometer, measuring full spectra of incident light. However, these devices are costly and inaccessible. Thus, CIE XYZ values measured from widely accessible hand held illuminance color meter was used to analyze accuracy of captured light spectra by a camera. As a background information, various color spaces are explained in Section 4.2.3.i. Calibration of HDR color images are explained in Section 4.2.3.ii based on this foundation.

i. Representing Color

CIE (Commission Internationale de L'eclairage – International Commission on Illumination) adopted XYZ color space to represent standard human colorimetric vision. It is a mathematical system of representing color within trichromatic human color vision for 2° and 10° visual fields. Different means of representing trichromatic color spaces are explained in this section.

a) LMS

In section 2.2., spectral sensitivity of photoreceptors was discussed. Each type of photoreceptors contains photopigments that has different absorption sensitivity to incoming photons. The three types of cones (S,M,L) are each sensitive to specific range of wavelength. S cones are most sensitive to the short wavelength, peaking around 450nm. M and L cones have peak sensitivity around 525 and 575 nm respectively.[16] Combination of different cone types allows full spectrum color vision.
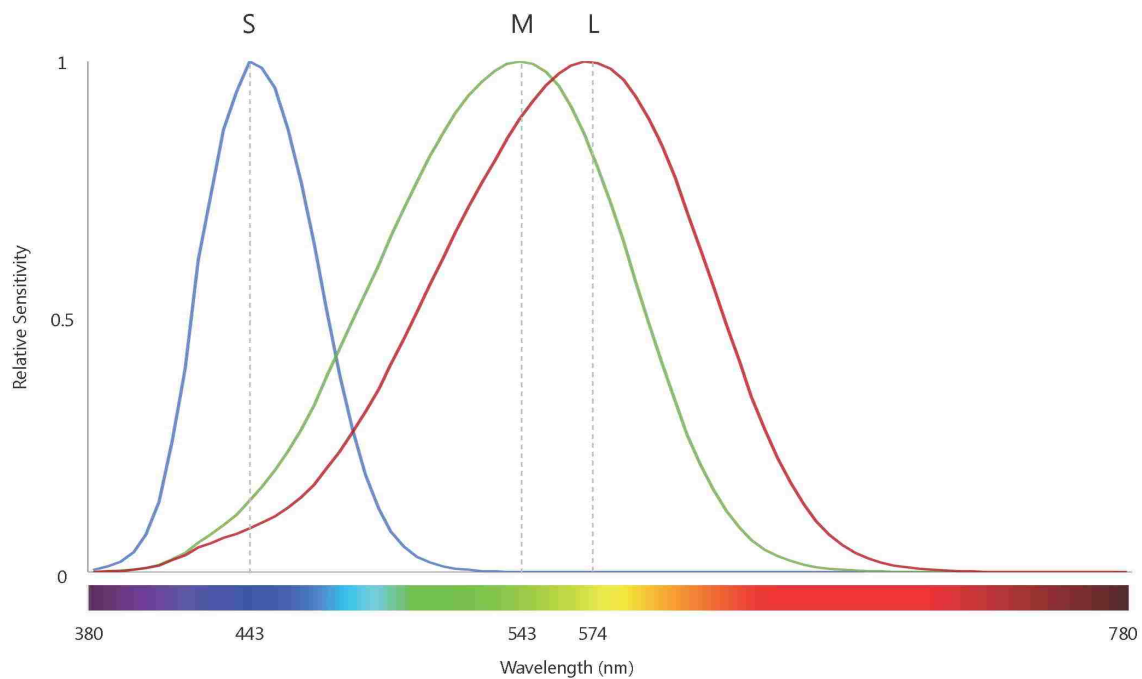
Figure 4.5. LMS color space

b) CIE RGB

As the spectral sensitivity for photopigments could not be figured out with sufficient accuracy during the 1920s, the CIE adopted a set of standard color matching function; CIE 1931 Standard

Colorimetric Observer. This is mathematical means of identifying any color within human color vision and is based on color matching experiments.[113][114] Color matching experiment is based on the concept of metamerism; stimuli with different spectral properties can be perceived as same color when it produces the same cone signals. The basic principle is to find out which combination and intensity of primary colors are required to match a specific color in visible spectrum.

As humans are trichromat, i.e., perceive color through three cones, where entire spectrum of incident light is reduced to three signals in the retina, three RGB monochromatic primary colors were selected for color matching experiment. Participants in the color matching experiment tries to match the test light color by changing intensity of primary colors shown in bipartite screen with 2° visual field. Any primary colors could have been selected as long as any one of the primary stimuli could not be matched by the other two stimuli. The selected RGB primaries were 700 nm, 546.1 nm and 435.8 nm respectively, chosen specifically for convenience of replicating the experiment and fabricating visual colorimeters. Resultant color matching functions are known as $\bar{r}(\lambda)$, $\bar{g}(\lambda)$, $\bar{b}(\lambda)$. They are scaled to yield equal energy stimulus with unit radiant power and defines spectral tristimulus values for chosen set of primaries.[115]
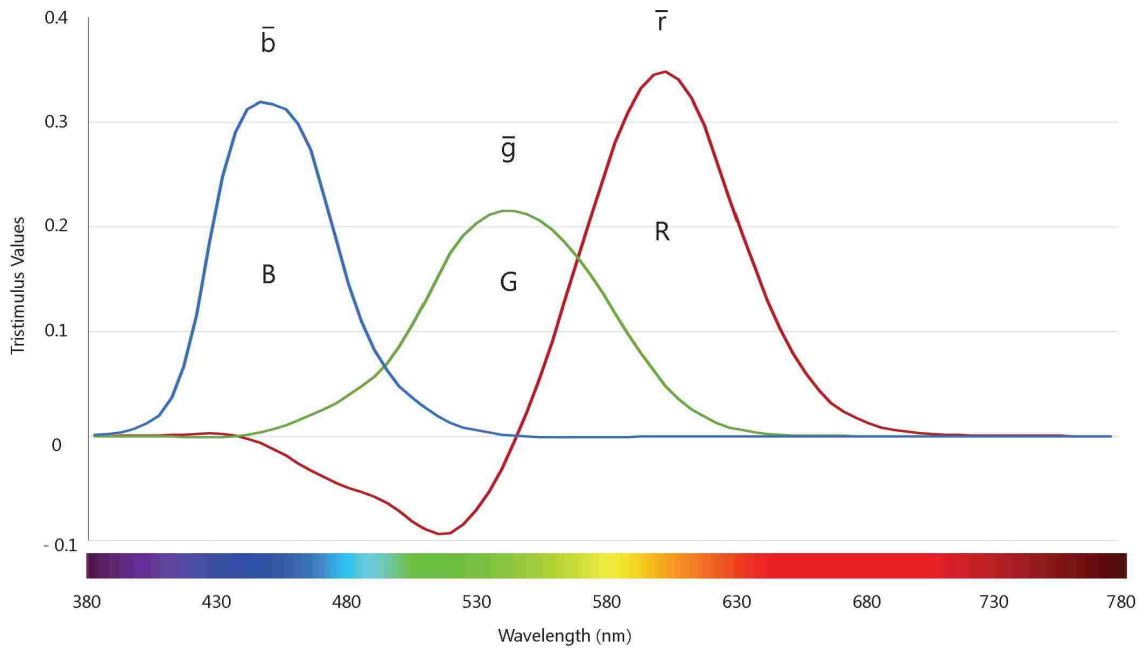
RGB tristimulus values for a stimulus with spectral power distribution S(λ):

$$R = \int_{380}^{780} S(\lambda)\,\bar{r}(\lambda)\,d\lambda$$

$$G = \int_{380}^{780} S(\lambda)\,\bar{g}(\lambda)\,d\lambda$$

$$B = \int_{380}^{780} S(\lambda)\,\bar{b}(\lambda)\,d\lambda$$

Figure 4.6. CIE RGB tristimulus color space

This CIE RGB system has negative values where $\bar{r}(\lambda)$ denotes subtraction of red primary stimuli to match the test stimulus. In other words, red primary stimulus had to be added to the test stimulus for color match. Negative values were inconvenient for calculation and instrumentation. Thus, a second colorimetric system was created through linear transformation: CIE XYZ system.

c) CIE XYZ

CIE XYZ system was created based on CIE RGB system. As with CIE RGB system, CIE XYZ system is devised for 2° visual field. New set of primaries were selected to create positive color matching functions of $\bar{x}(\lambda)$, $\bar{y}(\lambda)$, $\bar{z}(\lambda)$. Moreover, $\bar{y}(\lambda)$ function was selected to define CIE 1924 standard photometric observer function, $V(\lambda)$. Thus, calculation of photopic unit is equal to calculation of Y. Due to these requirements, the resulting primary stimuli are not physically realizable. CIE XYZ system conveniently combines color matching function and luminance function into a single system. Calculation of CIE XYZ values is same as calculation of illuminance or luminance; by weighting spectral power distribution curve of incident light with color matching functions, $\bar{x}(\lambda)$, $\bar{y}(\lambda)$, $\bar{z}(\lambda)$.
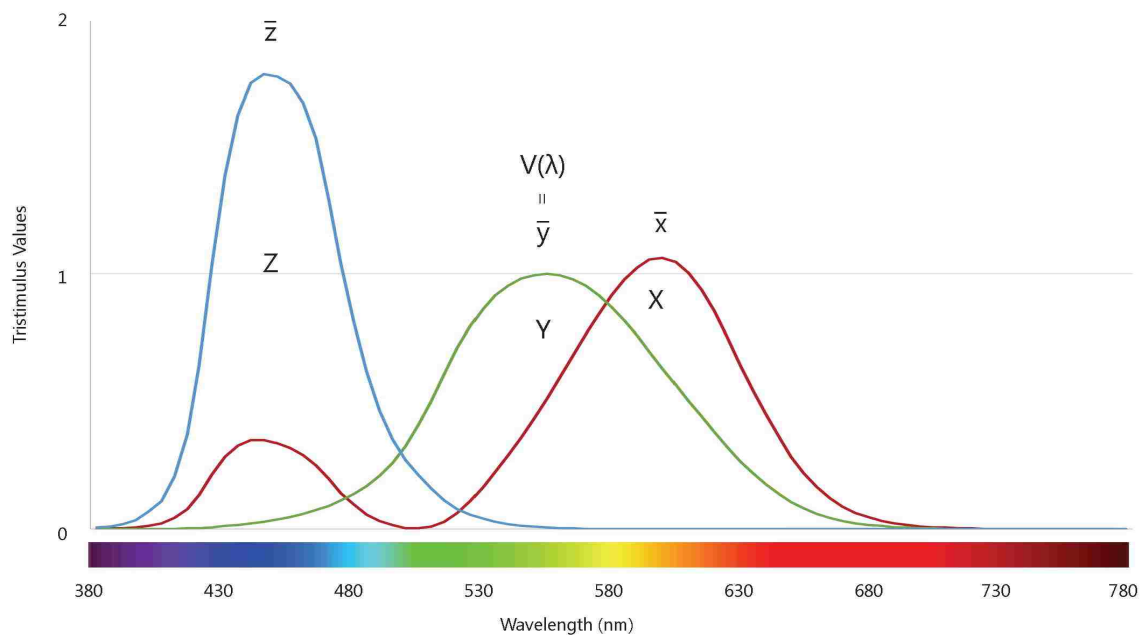
Figure 4.7. CIE XYZ system

XYZ tristimulus values for a stimulus with spectral power distribution S(λ):

$$X = \int_{380}^{780} S(\lambda)\, \bar{x}(\lambda)\, d\lambda$$

$$Y = \int_{380}^{780} S(\lambda)\, \bar{y}(\lambda)\, d\lambda$$

$$Z = \int_{380}^{780} S(\lambda)\, \bar{z}(\lambda)\, d\lambda$$

Both CIE RGB and CIE XYZ system represents color in a three dimensional space, describing luminance as well as chromaticity. Chromaticity of CIE XYZ system is represented and reduced to a two dimensional space with CIE Chromaticity coordinates. Coordinates for X,Y and Z are calculated through fraction and labelled as CIE chromaticity coordinates x, y and z respectively. Sum of x, y and z equals to 1; thus, only x and y is shown for two dimensional representation in CIE Chromaticity diagram. Third dimension representing luminance is also plotted in figure 4.8 b).
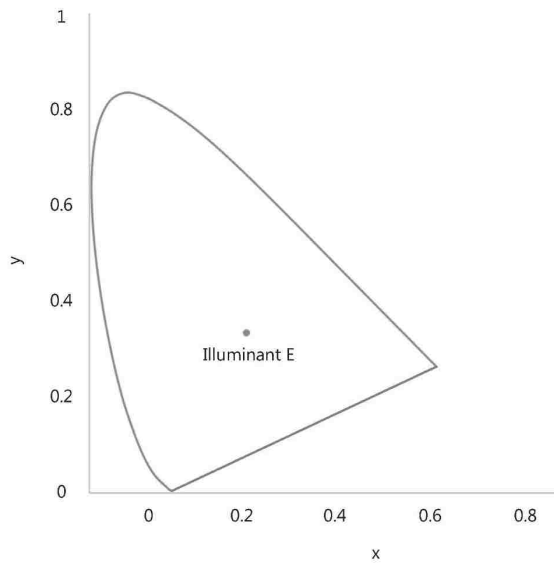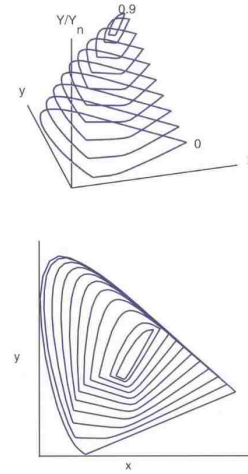
$$x = \frac{X}{X+Y+Z} \qquad\qquad y = \frac{Y}{X+Y+Z} \qquad\qquad z = \frac{Z}{X+Y+Z}$$

$$x + y + z = 1$$

Figure 4.8. Representing CIE xy

a) CIE 1931 chromaticity diagram (x,y)

b) 3rd dimension added to CIE chromaticity diagram [116]

d) Correlated Color Temperature (CCT)

CCT is the temperature of a blackbody (Planckian) radiator whose chromaticity most closely resembles that of the light stimulus under equal brightness and specific viewing condition. Planckian radiators are defined as a source that emits equal energy radiation. CCT is measured in Kelvin (°K) varying from red (~2000°K) to blue (~25000°K). It can be plotted on the CIE 1931 chromaticity diagram. (Fig. 4.9) All the colors of CCT are plotted on to a curve called Planckian locus. This further reduction of dimension in describing color (full spectrum – XYZ – xy – CCT) has its limits. First, it is a measure of describing perceived color, thus does not contain any information regarding spectral power distribution. Therefore, color render of an object from two separate light sources with same CCT may look different than the other due to different spectral content. Second, although CCT can be calculated from any chromaticity coordinates, it's result is only acceptable when the light source spectra resemble the Planckian radiator. In other words, CIE xy values must fall within close limits of Planckian locus. CCT measurements in this research is calculated from CIE xy using McCamy Method.[109]
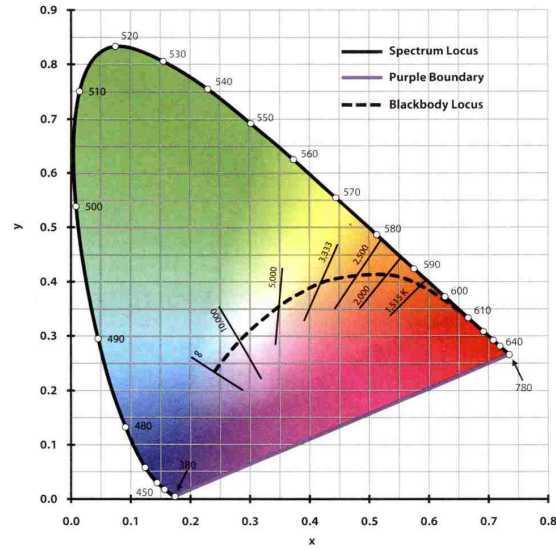
Figure 4.9. Representing CCT on plankian locus [16]

Calculation of CCT using McCamy Method [109]

$$n = (x - 0.3320) / (y - 0.1858)$$

$$CCT = 437 \times n^3 + 3601 \times n^2 + 6861 \times n + 5514.31$$

e) sRGB

Standard RGB (sRGB) is a system of describing color within digital production system. Digital devices generate color through three (R,G,B) phosphors. They act as primary stimuli to determine the color of a pixel. Chromaticity of these phosphors (primary stimuli) varies for different output devices and color systems. This limits the range of achievable colors, only showing subset of colors within the human color vision. (Fig. 4.10.) This range of achievable colors is known as a color space and defines the gamut (achievable colors) of the color space. There are various other color spaces in the digital production color system such as Adobe RGB with different gamut and chromaticity of RGB. sRGB was developed based on the average performance of personal

53

computer displays, and is the main color system used today. Similar to any other three dimensional color space, sRGB values can be transformed into the CIE XYZ Standard Color Observer.

Color spaces specifies an illuminant white point which defines the chromaticity of a light source for reference viewing environment. sRGB white point is defined as illuminant D65, which is typical monitor display viewing conditions (x = 0.3127, y = 0.3291). Therefore, the color white in sRGB color space will have chromaticity of D65 in reference viewing environments. Other color spaces define different reference white point. For example, CIE RGB specified white point as illuminant E (x = 1/3, y = 1/3). White point reference illuminant is used for mathematical transformation from sRGB to CIE XYZ or vice versa by scaling Y weighted with reference illuminant to 1.

54
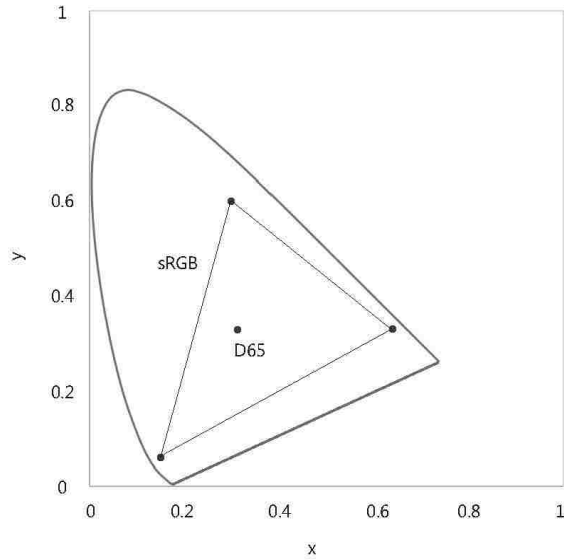
Conversion of sRGB values to CIE XYZ values

$$\begin{bmatrix} R \\ G \\ B \end{bmatrix} = \begin{bmatrix} 0.4124 & 0.3576 & 0.1805 \\ 0.2127 & 0.7151 & 0.0722 \\ 0.0193 & 0.1192 & 0.9505 \end{bmatrix} \begin{bmatrix} X \\ Y \\ Z \end{bmatrix}$$

Conversion of CIE XYZ values to sRGB values

$$\begin{bmatrix} X \\ Y \\ Z \end{bmatrix} = \begin{bmatrix} 3.2406 & -1.5372 & -0.4986 \\ -0.9689 & 1.8758 & 0.0415 \\ 0.0557 & -0.2040 & 1.0570 \end{bmatrix} \begin{bmatrix} R \\ G \\ B \end{bmatrix}$$

Figure 4.10. sRGB gamut on CIE 1931 xy chromaticity diagram / Conversion matrix for sRGB to CIE XYZ and vice versa [117]

ii. CIE XYZ and sRGB calibration

This section explains how to calibrate HDR photographs to closely match the light spectra of reality from measured CIE XYZ values. Camera and illuminance color meter captures incident light in different format. Camera captures light in sRGB values, while illuminance color meter measures CIE XYZ values. Therefore, to compare the captured values with the measured values, one format has to be converted to the other or vice versa. Thus, there are two methods of calibration. First, is by converting sRGB values from the HDR images to CIE XYZ to compare with the measured CIE XYZ values. Second is to do the reverse, by converting measured CIE XYZ values to sRGB values to compare with the sRGB values from HDR image. First method is called XYZ calibration and second, RGB calibration.

a) XYZ calibration

Both calibration methods require post processed HDR photographs following the methodology described in section 4.2.2. From these images, pixel sRGB values are extracted through Radiance pvalue command. For XYZ calibration, these sRGB values are converted to CIE XYZ values using simple matrix multiplication shown in figure 4.10. Then, each CIE X,Y and Z pixel values were represented as HDR images. The circular area of a fisheye image correspond to the 180° hemispherical data collection from a photometric device (Fig.4.11.). The mean value in the circular area is multiply by π to derive integrated XYZ values. This computation was done using a Python script to calculate the pixel mean of CIE X,Y and Z values.

56

CIE X

μ from HDR = 3043

CIE Y

μ from HDR = 3180

CIE Z

μ from HDR = 4005

Measured CIE X from color meter

= 2990

Measured CIE Y from color meter

= 3180

Measured CIE Z from color meter

= 2997
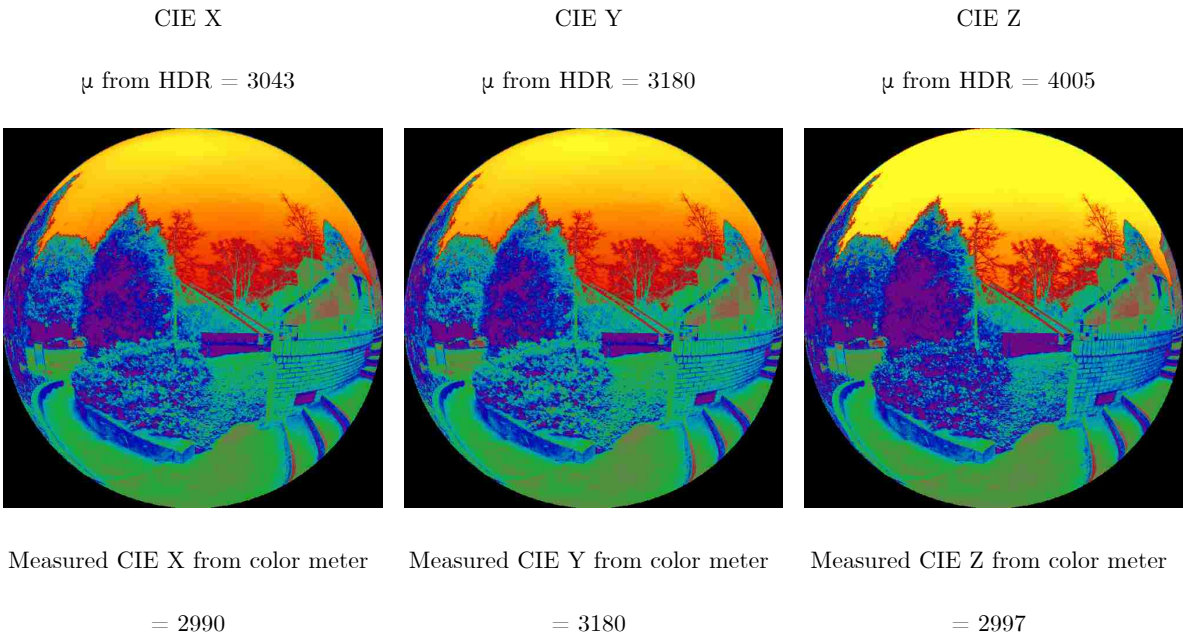
Figure 4.11. Captured CIE XYZ values measured from HDR images

Lastly, measured and captured CIE XYZ values from 70 HDR images were plotted against each other (Fig. 4.12). These 70 images provide diverse lighting conditions with daylight and electric lighting. The minimum and maximum illuminance values range between 20 and 12640 lx. The minimum CCT values range between 2500°K and 15000°K. The plot showed linear relationship for all X, Y and Z data. Line of best fit was calculated using the least squares method. Intercept was forced through the origin to match the ideal condition, where measured values and captured values had 1 to 1 relationship. Regression showed Z values were over estimated whilst X and Y values demonstrate an almost 1 to 1 relation.

Figure 4.12. Measured and captured CIE XYZ values relation plot of 70 HDR photos

Regression line equation and R^2 (coefficient of determination) value for X, Y and Z data plot

X = 1.01288025 x   Y = 1.00062068 x   Z = 1.28723957 x

$[R^2 = 0.99994]$ $[R^2 = 1]$ $[R^2 = 0.998]$

To calibrate the captured values from the camera to have 1 to 1 relation with the measured values, both X and Z values required calibration. However, only Z values were calibrated as X was close to 1 to 1 relationship. Another assumption was made that B channel accounted for all differences in Z values (although Z values covers both B and G wavelengths, it peaks mostly in the B wavelengths). Based on these assumptions, calibration coefficients for B channel is shown below.

$B_{calib} = 0.77688005 * B$

$G_{calib} = G$

$R_{calib} = R$

58

Based on these calibration coefficients for sRGB, consequent calibrated CIE XYZ is as follows.

$X_{calib} = 0.91022685 * X$

$Y_{calib} = 0.98389074 * Y$

$Z_{calib} = 0.87692449 * Z$

This CIE XYZ calibrated coefficients demonstrate a problematic approach as calibrated Y value does not match to the original values. Calibrated Y (photopic unit) should have 1 to 1 relation to original Y, as HDR images were calibrated with illuminance measurements (measured Y values from illuminance color meter). Therefore, to provide consistency, G channel was also calibrated. Calibration coefficients for B and G is as follows.

$B_{calib} = 0.77688005 * B$

$G_{calib} = 1.02252728 * G$

$R_{calib} = R$

And consequent calibrated CIE XYZ is as follows.

$X_{calib} = 0.96610479 * X$

$Y_{calib} = Y$

$Z_{calib} = 0.80772244 * Z$

This calibration method required various assumptions. Therefore, it does not present a straightforward methodology. Another methodology is presented below.

b) RGB calibration

The second method of spectral calibration is RGB calibration. This is more straightforward calibration method as calibration coefficients for sRGB is calculated directly, rather than trying to calculate sRGB calibration coefficients from CIE XYZ coefficients. This means the calibration can be applied directly to the HDR photos, which uses sRGB format, for more precise calibration. Measured CIE XYZ values are converted to sRGB values using standard color space (sRGB) reference primaries (Fig 4.10). Like the first method, mean sRGB values are calculated after extracting pixel sRGB values and mean values are multiplied by π to derive the integrated values over an 180° hemispherical projection to match the area seen by the Konica Minolta CL-200A illuminance color meter. Finally, these measured and captured sRGB values are plotted against each other (Fig. 4.13).
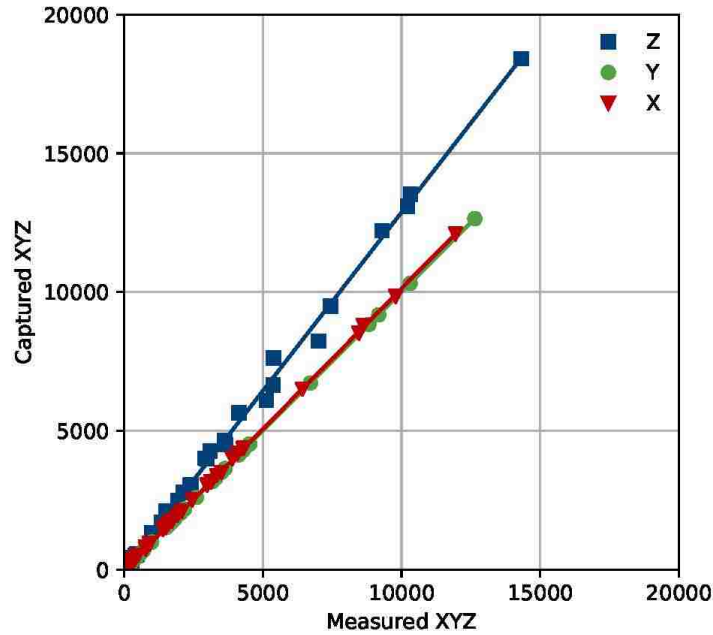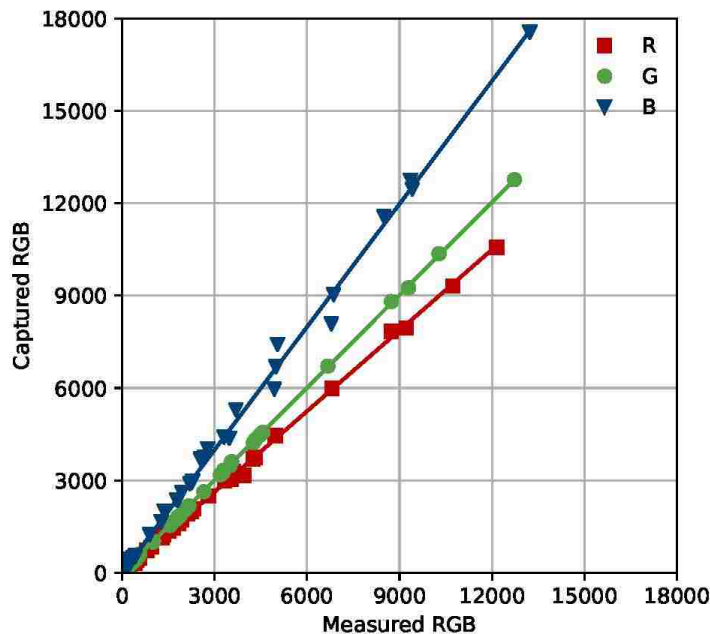

Figure 4.13. Measured and captured sRGB values relation plot of 70 HDR photos

60

Regression line equation and R^2 (coefficient of determination) value for R, G and B data plot

R = 0.87433556 x   G = 1.00222207 x   B = 1.33079957 x

[R^2 = 0.99721]   [R^2 = 0.99995]   [R^2 = 0.99922]

sRGB regression showed that the camera was over estimating B channel whilst underestimating R channel. G channel had almost 1 to 1 correlation. From this data, simple correction was applied to align the measured and captured data. Correction coefficients for sRGB is as follows.

R_{calib} = 1.14377216 * R

G_{calib} = 0.99780483 * G

B_{calib} = 0.75142771 * B

Consequent CIE XYZ is shown below.

X_{calib} = 0.9641393 * X

Y_{calib} =1.01106365 * Y

Z_{calib} = 0.85524518 * Z

As a result of this calibration technique, sRGB calibration coefficients are aligned between the captured and measured sRGB values. Also, measured XYZ values match closely with calibrated XYZ values from the image. Melanopic luminance is calculated using calibrated RGB values.

4.3. Photopic and Melanopic luminance calculation

Calibrated HDR photos can be used to calculate both photopic and circadian luminance. Using sRGB primaries and V(λ), Photopic luminance (P_L) is calculated as;

$$P_L = 179 * (0.2121 * R + 0.7166 * G + 0.0713 * B) \ (cd/m^2)$$

The coefficients for R, G and B equals to the area under the curve between sRGB interval.
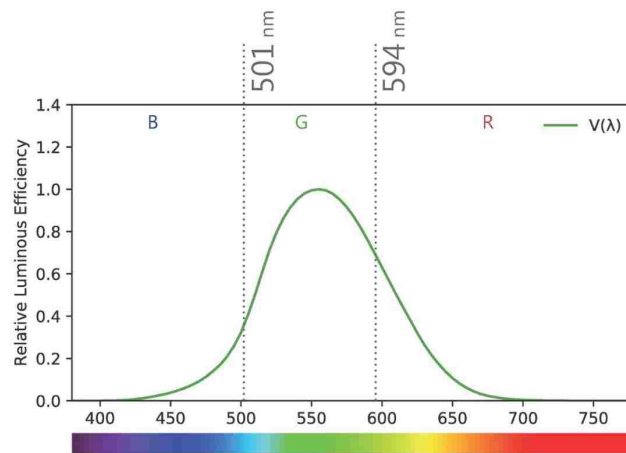
Figure 4.14. V(λ) with sRGB intervals

The interval for sRGB is derived by calculating the area under the normalized V(λ) within the interval wavelength and checking to see if it equals to the coefficients. Using the same intervals, the coefficients for Melanopic luminance (M_L) can be calculated as;

$$M_L = 179 * (0.0013 * R + 0.3812 * G + 0.6175 * B) \ (cd/m^2)$$
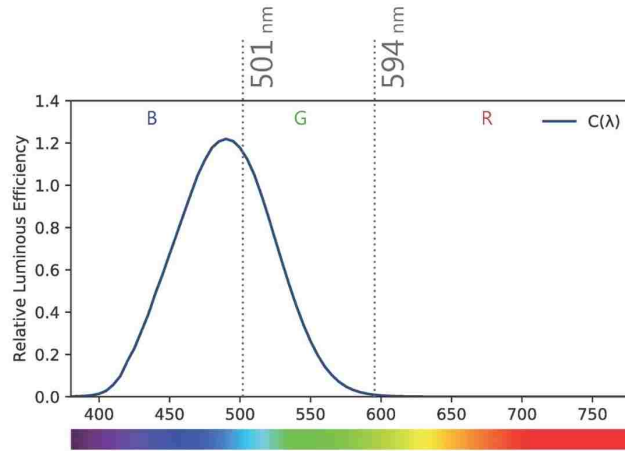
Figure 4.15. C(λ) with sRGB intervals

Using these two formulas, it is possible to calculate both photopic and melanopic units.
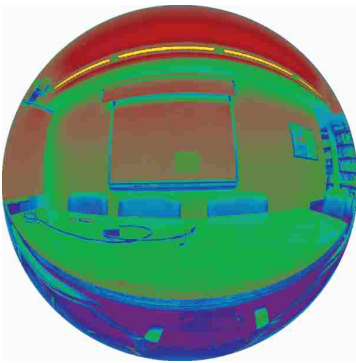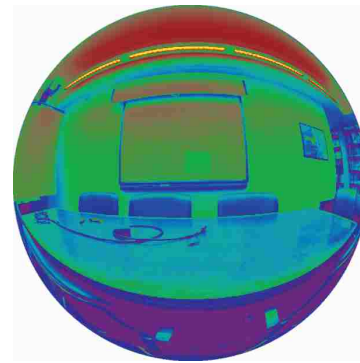
P_L = 179 * (0.2121 * R + 0.7166*

G + 0.0713 * B) (cd/m2)

(P_L * π = lx)

240 lx

M_L = 179 * (0.0013 * R + 0.3812*

G + 0.6175 * B) (cd/m2)

(M_L * π = lx)

135 lx

Figure 4.16. Calculating Photopic and Melanopic units

www.manaraa.com

5. Results

The data collection took place around greater Seattle area over a yearlong period. This collection period allowed for capturing a wide variation of conditions that included different sun positions, cloud cover, seasonal variations, electric lighting, indoor and outdoor settings, and varying views within different architectural context. The total number of HDR images collected are 250.
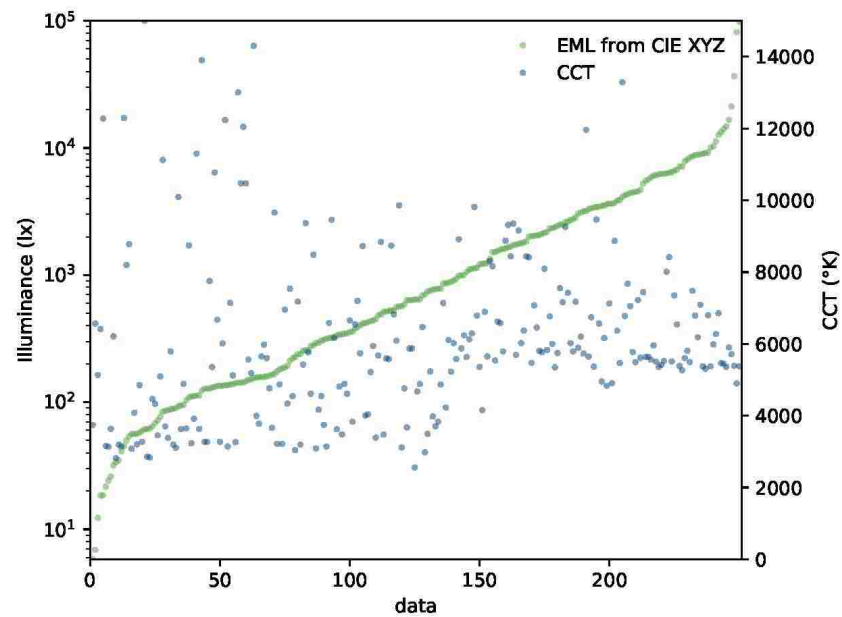
Figure 5.1. Variation of illuminance and CCT from collected data

In this section, calculated circadian light from captured HDR photos are discussed. The results shown here demonstrate the instantaneous photopic and circadian values as they are recorded at the time of photographic capture and colorimetric measurements. Before analyzing the results, it is important to note and reemphasize our abilities to interpret them is based on the state-of-the-

64

art photobiological research. As mentioned in section 2 and 3, the exact interaction of five photoreceptors in conveying light information to ipRGCs and consequent physiological responses in response to variation of intensity, duration and timing of light exposure is not well known. As a result, there is no standardized function combining the influence of all photoreceptors to consider timing, spectra, intensity, duration, photic history, spatial distribution and age. This mean s it is difficult to compare situations such as: long exposure to low circadian light levels and short exposure to high circadian light levels. Moreover, the impact of same circadian light exposure will vary for individuals depending on their personal photic history and age. In this study, timing, spectra, duration and intensity of light is considered but not personal photic history and age. It should also be noted that there is no consensus on metrics for measuring circadian light. This is due to lack of standards on the exact form of the circadian luminous efficacy function and agreement on scaling of the function. The reported units in this study may require update as metrics on circadian light develops.

Nonetheless, the results shown here are analyzed based on most recent guidelines and researches available to the author. The circadian efficacy function used in the study is developed by Lucas et al, reported in Equivalent Melanopic Lux (EML) or melanopic illuminance.[38] The efficacy function is weighted with pre-receptoral function of 32 year old. Lucas et al. recommends reporting light levels from all five photoreceptors due to lack of standardized function to combine the effect of all five photoreceptors. This study only reports light levels to melanopsin in EML as it plays predominant role in conveying light signals to ipRGCs in diurnal conditions. There is no restriction in reporting all values, as the methodology for calculating EML can be applied to other photoreceptors. However, without a methodology to process the five channel data in a consistent

manner, it is more straightforward to compare different lighting situations with one circadian unit. Threshold for minimum circadian light exposure is defined in reference to International WELL Building Institute's standard; 250 EML exposure for at least 4 hours of light exposure to entrain the circadian system.[70] Judgements on timing of light exposure is based on evidence that light exposure in early biological night (evenings) will delay circadian phase, whilst light in late biological night (early mornings) will advance circadian phase. Light exposure during mid day is known to increase alertness.

It is generally agreed higher intensity with spectrally blue rich light for longer exposure is more likely to trigger melatonin suppression and circadian phase shift. Depending on circumstances, it may be desirable to sync circadian rhythm with the natural day-night cycle from daylight as main source. For others - whose working hours do not follow the normal day-night cycle - it will be better to sync circadian rhythm to match personal working hours from electric lights. Results in this section is interpreted for the majority of the population whose circadian rhythm should sync with day-night cycle. In the first section of this chapter, captured point in time scenes from various built environments is discussed to outlines some factors that affects variability and quantity circadian light.

5.1. Point In Time Analysis

5.1.1. Influence of Built Environments

For many people, various factors influencing circadian rhythm (spectra, timing, intensity of light) is defined by the restraints and affordances of built environments. Architectural features such as size and orientation of openings, glass color and transmittance, surface materials, furniture

orientation, spectra and intensity of electric light sources are design decisions that impact the luminous environment. The resulting building shapes the lighting experience for its occupants, and determines both the photopic and circadian light exposure. The following examples in figure 5.2 shows how some of these design decisions greatly impacts circadian light.

Outdoor environments in figure a) shows high photopic and melanopic illuminance well above 3000 lx compared to indoor conditions. In comparison, light intensity drops considerably when indoors for both photopic and circadian systems. Spectra of light, view orientation and light intensity determines the amount of melanopic light. For instance, scene from b) and c) were taken within on a same spot around the same time in an office. The only variation was orientation where scene c) was captured 90° rotated from scene b). Spectra of light within these scenes and resulting CCT is very different. Scene b) has blue rich light from daylight entering from the window, whilst scene c) is looking at low CCT electric light. In both scenes photopic illuminance is around 240 lx. However, due to spectra of light for each scene, circadian light is reduced by almost 50% in scene c). Intensity of light also plays a direct role in circadian light exposure.

Scene d) is a basement office space for an IT technician. Due to the scope of work requiring long durations looking at the computer screen, the occupant of the office prefers to keep the light levels low. It can be clearly seen that as photopic light is extremely low, circadian light is also very low compared to other scenes. To stimulate circadian system in this circumstance, combination of higher intensity and higher blue content of electric light would be required. However, as light serves dual purpose for both visual and non-visual activity, solution is not easy. To achieve 250 EML, as recommended by the WELL Building Standard, the occupant can raise the light levels.

However, it is likely the occupant wants to keep the light levels low due to the scope of the work. In which case, blue rich light is required. However, regardless of blue rich light spectra, it will be difficult to achieve 250 EML from low illuminance levels such as 22 photopic lx. This is where duration of light exposure will come into the equation – only, the exact duration of exposure to equal 250 EML for 4 hours in this light condition is not known. As having enough circadian light exposure during the morning is more effective than in the afternoon, the occupant could raise the light levels in the morning and dim in the afternoon. Yet, alertness of the occupant will be affected in lower light conditions. Moreover, if the occupant's photic history is not synced to current time zone, he/she will be more sensitive to higher EML compared to one who is synced to current time. Spending time outdoors (or in well-lit indoor spaces) in the morning and throughout the day during morning commute and frequent breaks during the day may help to address the problem. As explained in this paragraph, determining and adjusting circadian lighting and integrating with visual light experience is not simple.

Time	11:22 am	11:29 am	11:33 am	2:27 pm
Date	May 4	May 4	May 4	May 4
	(a)	(b)	(c)	(d)

Measured CCT				
	5495 K	7176 K	3192 K	3157 K

Photopic fc				
	8413 lx	238 lx	240 lx	22 lx

Melanopic fc				
	7884 lx	258 lx	135 lx	13 lx

1 5 14 36 109 326 973 3000 cd/m²
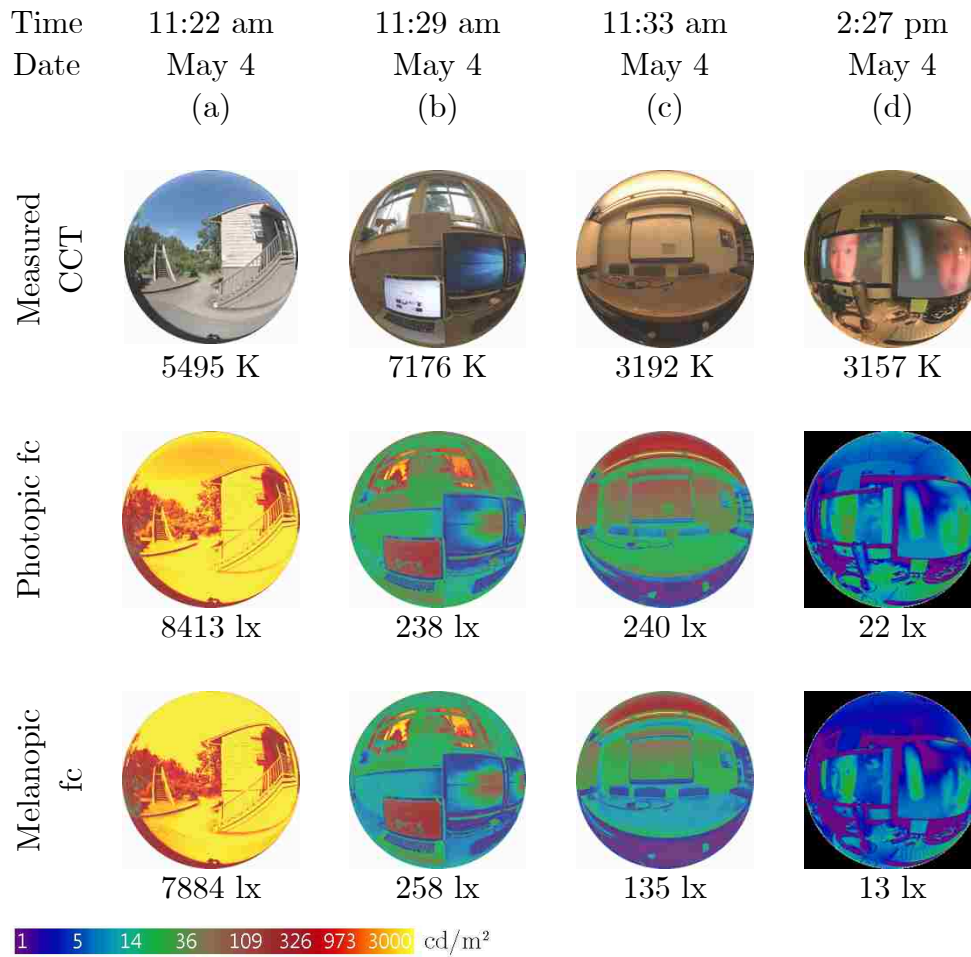
Figure 5.2. Variation of photopic and melanopic illuminance depending on architectural context

HDR photos taken on May 4th.

5.1.2. Influence of Weather

In environments where daylight is the main source of light, controlling circadian light gets more complex due to external influences such as weather. Figure 5.3. shows 4 scenes taken with same view on two different dates. a) and b) were taken on April 15th at around 1:30 pm and 4:30 pm, while c) and d) were taken on May 4th around the same times. For scenes in April, clear sky conditions persisted with high light levels. Due to clear blue sky visible in majority of the scene, CCT is high - raising circadian light levels higher than photopic light. A graph was plotted to find out what CCT raised circadian illuminance levels above photopic illuminance levels. Plot for all captured data showed circadian illuminance rose higher than photopic illuminance at around 6000°K. This is certainly not a definite number to indicate what CCT the light should be to raise circadian illuminance. As explained in section 4.2.3.i.d, CCT does not represent spectra of light and should only be used as an indicator for perceived color. Electric light sources with inconsistent spectra will have different spectral content to daylight despite having same CCT.

Weather in May scenes were more dynamic. Scene c) shows a clear sky condition whilst d) shows an overcast condition. False color images for two scenes shows that weather influences not only affect the intensity of light, but also the spectra. Light in scene d) is low for both photopic and melanopic light. It would be hard to perform fine visual tasks with 150 photopic lx, and it would not entrain the circadian system. Considering the scene was taken in the afternoon, it is preferable to keep circadian light levels low.

Time	1:31 pm	4:32 pm	1:22 am	4:29 pm
Date	April 15	April 15	May 4	May 4
	(a)	(b)	(c)	(d)

Measured CCT				
	7423 K	9162 K	7159 K	5979 K
Photopic fc				
	2615 lx	1766 lx	2498 lx	158 lx
Melanopic fc				
	2822 lx	2029 lx	2727 lx	151 lx

| 1 | 5 | 14 | 36 | 109 | 326 | 973 | 3000 | cd/m² |
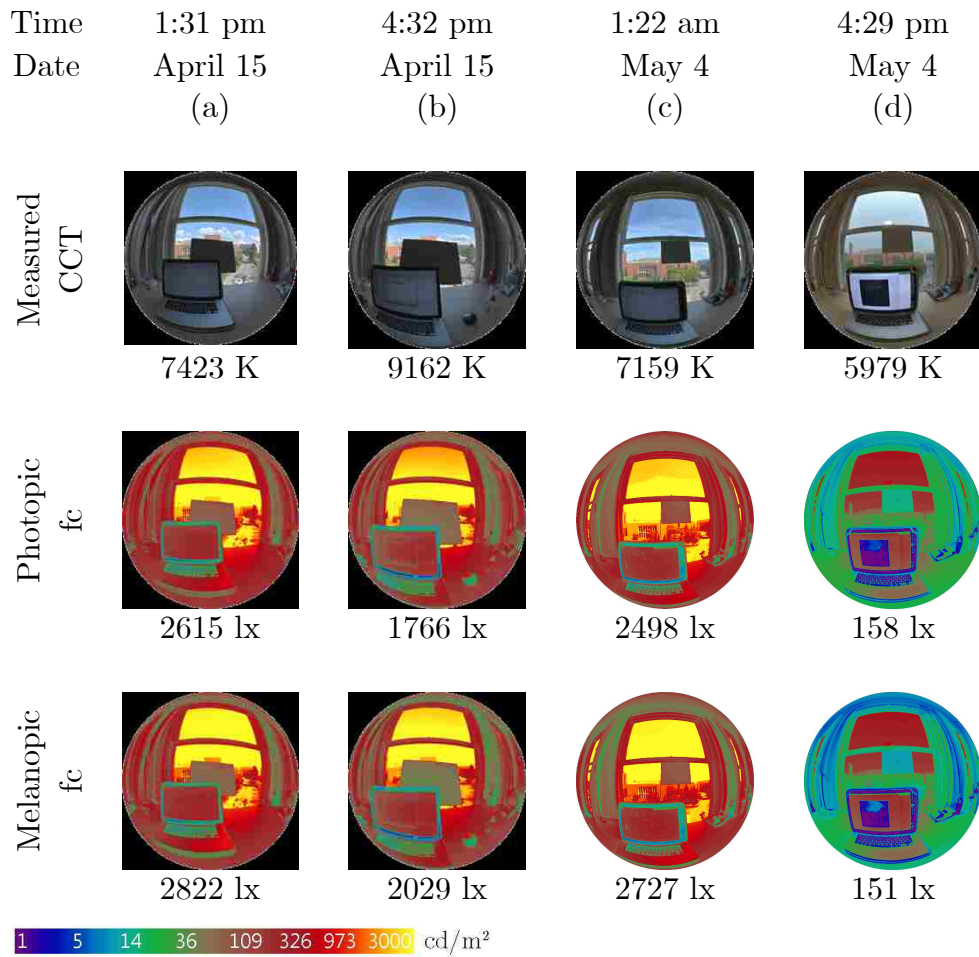
Figure 5.3. Variation of photopic and melanopic illuminance depending on weather

HDR photos captured on May 4th and April 15th at around 1:30 pm and 4:30 pm with different weathers in the latter.
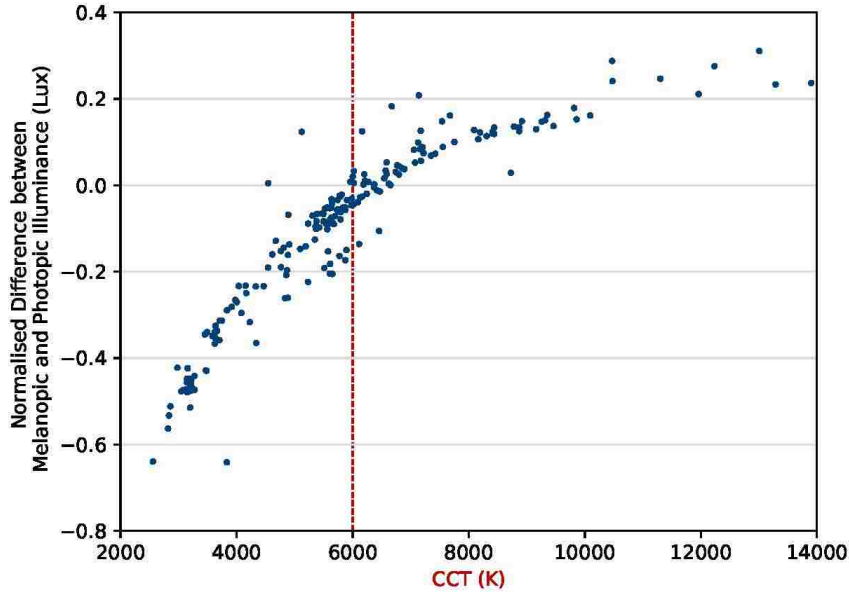
Figure 5.4. Relationship between CCT, photopic and melanopic illuminance
At around 6000°K melanopic illuminance rises higher than photopic illuminance

5.1.3. Influence of Building Depth

As explained in section 5. ii, built environments has a lot of influence in shaping the light experience of the occupant. This section shows some examples on how building depth influences circadian lighting experience. Figure 5.5 shows four HDR photos taken around the same time in a space with large glazing on overcast day. The only variable is distance to the glazing with scene a) being closest and d) being furthest away from glazing. HDR photos show light level dropping progressively with increasing distance. Figure a) shows scene for an individual sitting in front of window in the café area. High photopic and melanopic light is reached to the cornea, raising alertness. For people seated further inside the area as seen in scene b), c) and d), less daylight is available due to decrease in visible sky (the main source of light intensity for both photopic and circadian light as seen in false color images). In scene d), supplementary electric light is seen, lighting the scene and accenting architectural features for visual recognition. Comparing photopic

72

and circadian false color images for scene d) shows electric light increases luminance for photopic system, but does little for the circadian system. This is mainly due to the spectra of the electric light used in this scene. With higher intensity and blue rich spectra, it could raise the circadian light levels. These scenes show potential of daylight as primary light source in delivering adequate light intensity and spectra to the circadian system. It also gives clues in organizing building programs to take full benefit of daylight for occupant health.

Time	1:27 pm	1:34 pm	1:37 pm	1:43 pm
Date	Aug13	Aug13	Aug13	Aug13
	(a)	(b)	(c)	(d)
Measured CCT	5793 K	5579 K	5676 K	5095 K
Photopic fc	2753 lx	932 lx	483 lx	77 lx
Melanopic fc	2582 lx	849 lx	440 lx	65 lx

| 1 | 5 | 14 | 36 | 109 | 326 | 973 | 3000 | cd/m² |
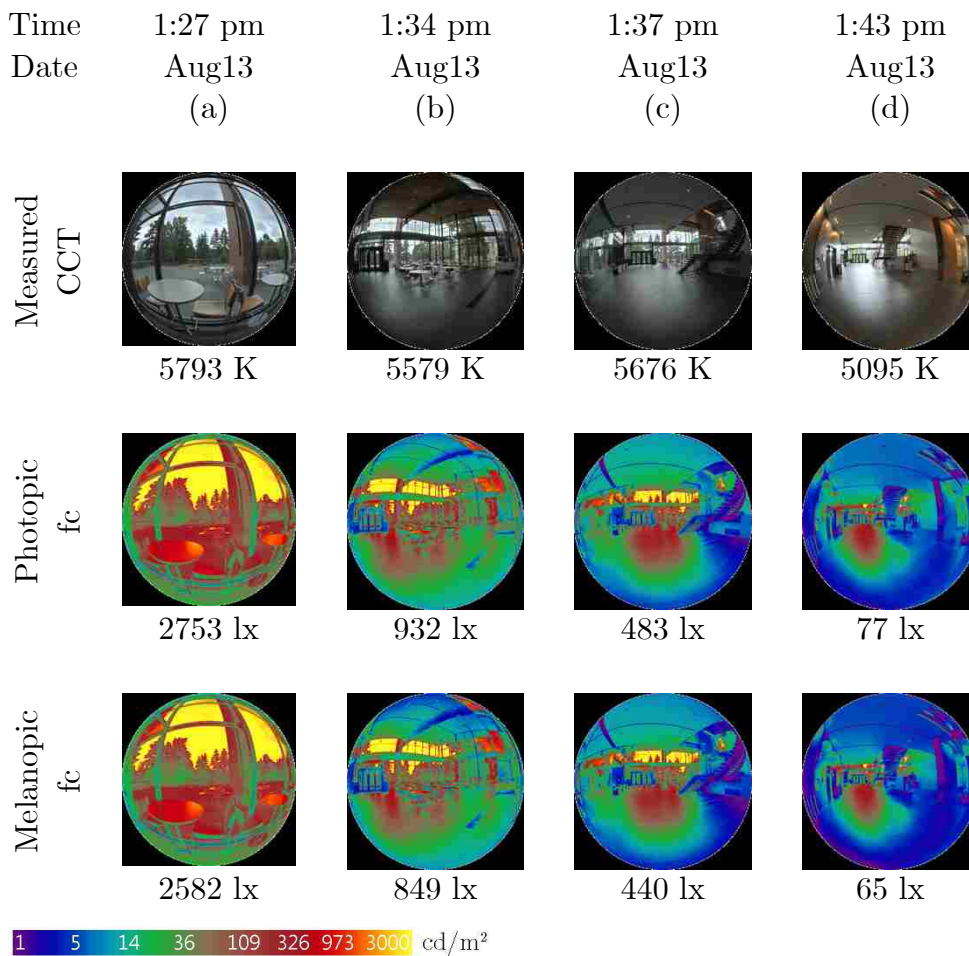
Figure 5.5. Variation of photopic and melanopic illuminance depending on building depth

73

5.1.4. Influence of View Direction

This section discusses influence of view direction on circadian light. Figure 5.6. shows outdoor scenes taken around noon on September 15th in sunny sky conditions. All scenes were taken on same spot with 90° rotation. Intensity and spectra of light changed greatly with differently views. Scene a) facing North had highest CCT with around 7000°K whilst other scenes were around 5000°K. Despite having highest photopic illuminance, scene c) facing South had smallest percentage increase in EML with 2%. Scenes a), b) and d) showed 5% increase. This can be attributed to yellow rich spectra of sunlight, lowering blue spectra of daylight for scene c). For these scenes, full spectrum measurements were also taken. In the previous section, 6000°K was mentioned as threshold for raising circadian light values above photopic light. This is generally observed, but its limitations should be noted. CCT is a single number and different spectral compositions of light may lead to the same CCT value (i.e. metamerism). Therefore, CCT cannot represent spectral information and it is limited in its ability to explain the relationship of the photopic and circadian values in a scene. The full spectral distribution of light or the CIE XYZ values provide better data. For instance, scenes b),c) and d) have lower CCT values than 6000°K. However, spectral power distributions for each scene clearly shows high values in the blue range due to daylight as the source. Depending on view direction there was 90% change in circadian illuminance in outdoor environments.

This percentage change becomes less drastic in indoor conditions. Figure 5.7 shows different photopic and circadian illuminance with varying view direction in an office environment. All three scenes were taken around same date and time in the same room with overcast conditions. a) shows scene looking at the back of a conference room. The occupant with this scene receives 130 EML,

74

which will not be enough to properly entrain the individual's circadian system with short time exposure. On the other hand, scene b) and c) shows plenty of light for both photopic and circadian light.
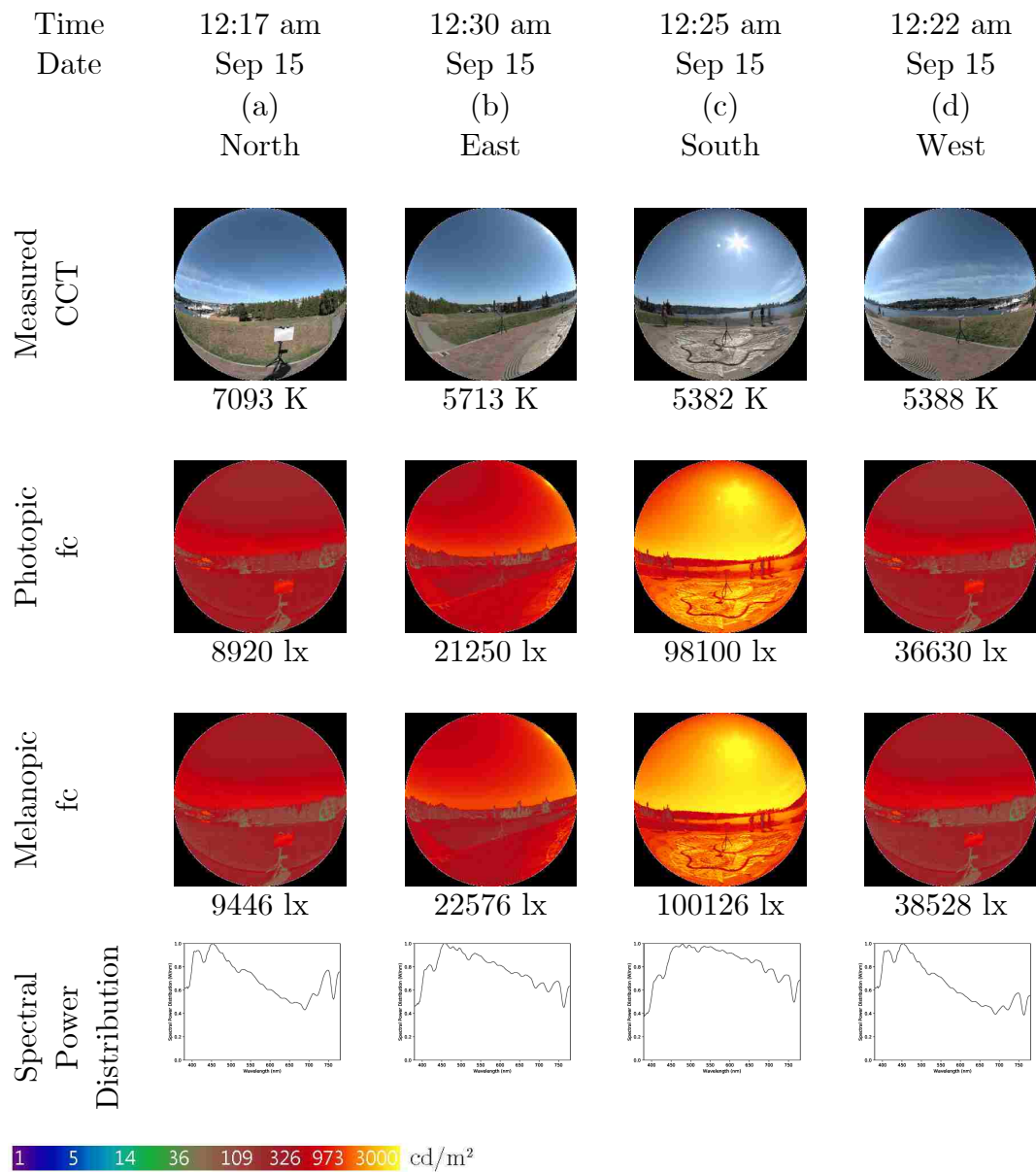
Figure 5.6. Orientation influence in photopic and melanopic illuminance - in outdoors environements

Time	11:17 am	11:30 am	11:25 am
Date	May 19	May 19	May 19
	(a)	(b)	(c)
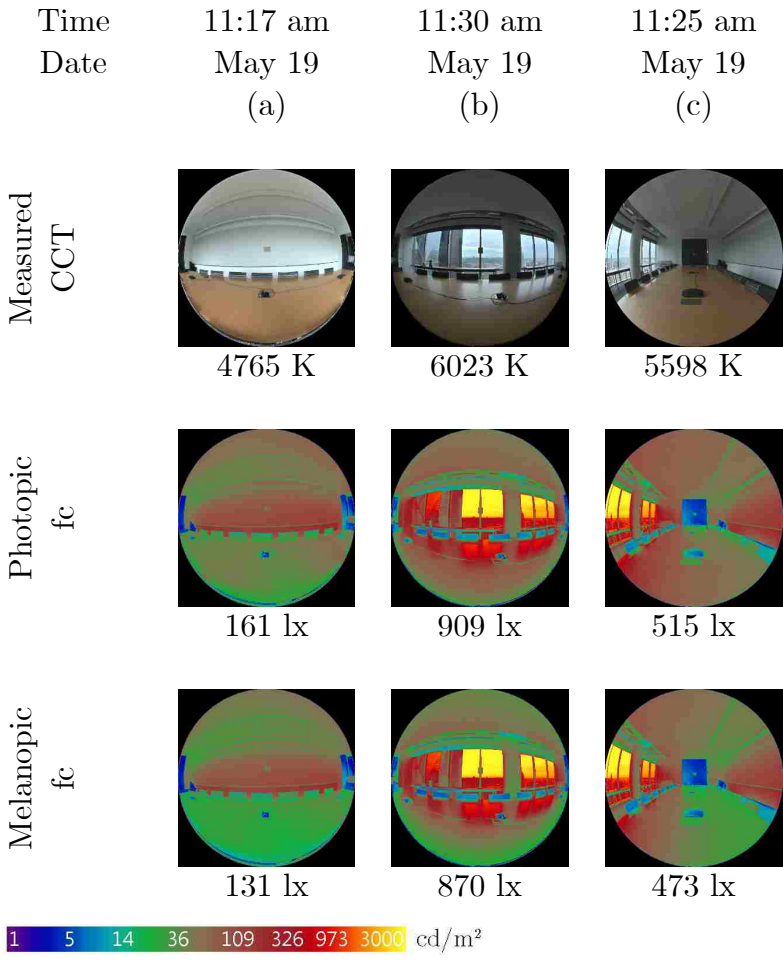
Figure 5.7. View direction influence in photopic and melanopic illuminance - in indoors environements

5.1.5. Influence of Light at Night (LAN)

Regulating LAN is very important as it delays circadian phase response by delaying melatonin secretion. This phase delay not only affects alertness for adult individuals, it is also extremely critical for growing children as nearly 50% of daily growth hormone is released during deep sleep phase.[118] Figure 5.8 shows four different night scenes. Scene a) and b) were taken in a room with different spectra of electric light. Scene a) has low CCT of around $3000 - 3500°K$ (typical indoor light) whilst scene b) has blue rich light of around $10000°K$. Both scenes has relatively similar photopic illuminance, but melanopic illuminance for scene b) with higher CCT has increased by

around 2.5 times due to spectra of light source. Scene c) and d) shows two different offices. Both scenes have similar CCT of 3000°K which decreased circadian illuminance by around 50% to photopic illuminance. However, scene d) has much dimmer light conditions further decreasing the circadian light. All scenes in figure 5.8 do not approach 250 EML, either due to low intensity of light, or due to lack of blue spectra. However, it must be noted again that duration of light exposure is not taken into account in this analysis. Longer duration with lower circadian light levels may induce full melatonin suppression as only 77 EML is required to trigger 50% melatonin suppression.[66] In general, it is advisable to keep light levels low at night with lights lacking blue spectra.
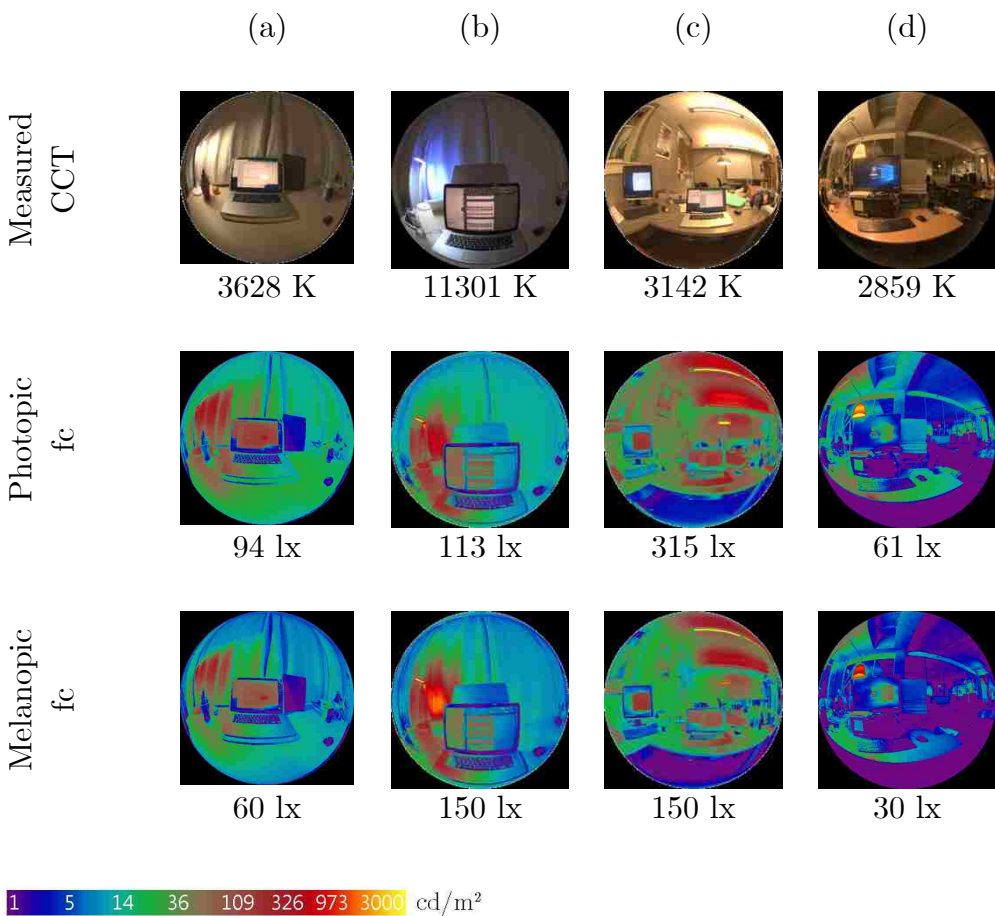
Fig 5.8. Variation of photopic and melanopic illuminance at night

5.2. Period Analysis

Point in time analysis is limited in terms of incorporating other factors such as duration. Period analysis provides more comprehensive overview of an individual's circadian light experience throughout a day. This makes it easier to predict entrainment of circadian system and alertness during the day. Figure 5.9 shows sequence of light conditions experienced by the author on February 25th. At 8 am, the author spent the morning in home environment with only daylight. Due to overcast sky conditions, proximity to a window and low CCT, circadian light levels were low. From 9 am to 1pm, the author spent a few hours in daylit home office environment. Primary view was to a window facing East. False color images show high light levels were coming from daylight. Circadian light levels were well above 250 EML for 4 hours, entraining the circadian system. At 1 pm, the author went outside to get lunch receiving even higher light exposure than in the morning.

Afternoon was spent in university office. The primary view was towards a wall with some daylight exposure from West facing window. Circadian false color images show considerably lower circadian light levels in the university office compared to the home office environment. This is mainly due to choice of view direction, size of window and building context. Home office was situated on 7th floor with no surrounding obstruction whilst university office was on the ground floor in close proximity to surrounding context. Circadian light levels progressively dropped with time in the university office, which is desirable in the afternoon to maintain circadian phase response. Effect of alertness is still hard to measure in period alertness as the exact required amount is not known. At 5 pm, around the sunset, the author went out to get dinner. Although CCT was high, light levels were low keeping circadian light levels lower than in the morning. At 6 pm, after sunset,

the author walked back to home in very low circadian light levels. If the author was not exposed to high levels of LAN, his / her circadian rhythm would have entrained closely to natural day-night cycle (Fig. 5.10).

Figure 5.9. Example day on Feb 25th in Seattle with high circadian light exposure
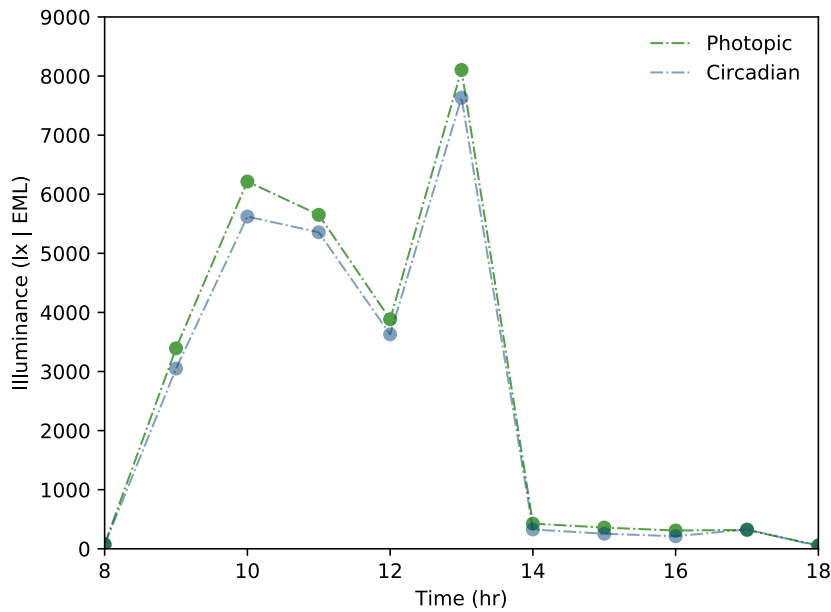
Figure 5.10. Variation of photopic and melanopic illuminance on Feb 25th with high circadian light

79

Figure 5.11 shows an example day for an individual who works in a window-less office. In contrast to the day experienced by the author as shown in figure 5.9, this person is exposed to very low light levels in the morning. He / she has to rely on circadian light exposure during morning commute and lunch time to entrain the system. Lunch time circadian light exposure is not ideal timing as lower circadian light is preferable in the afternoon. Alertness for this occupant is likely not high due to low light levels throughout the day (Fig. 5.12). It is still hard to judge whether high light levels for short duration as in this scenario is enough to entrain the system.
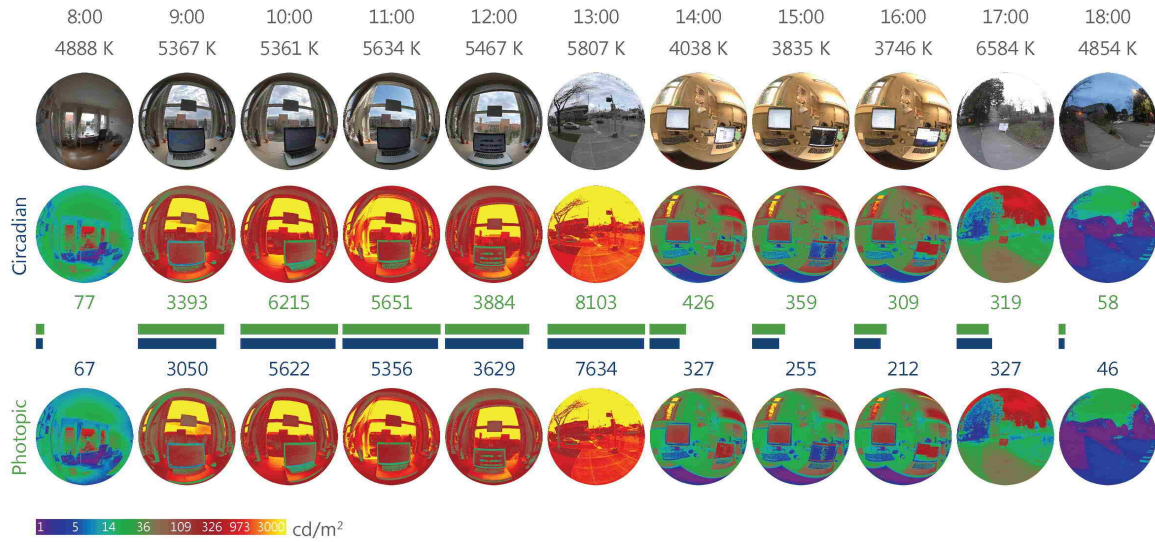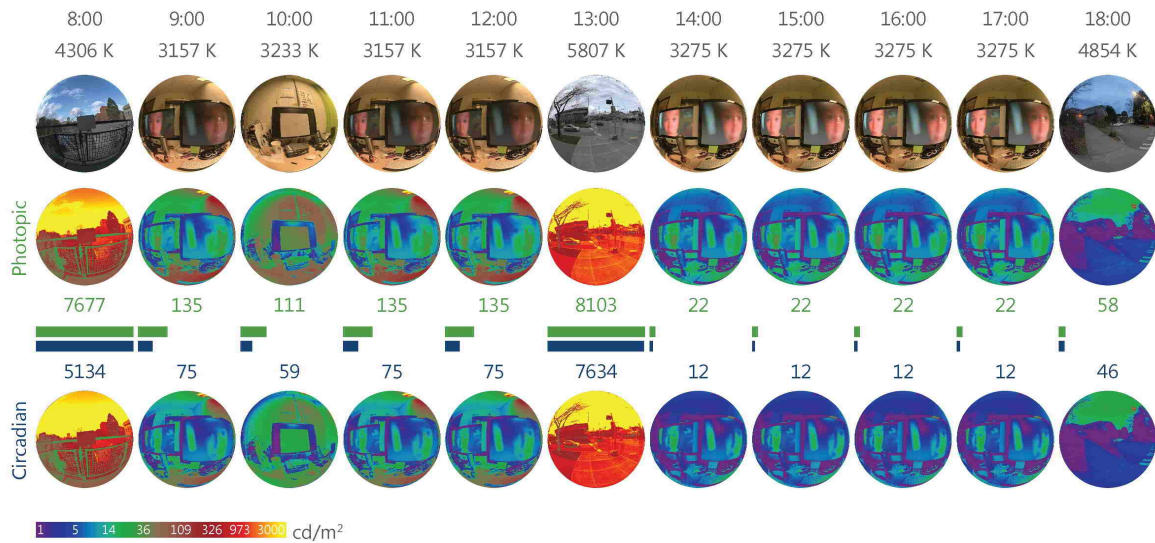

Figure 5.11. Example day on Feb 25th in Seattle with low circadian light exposure
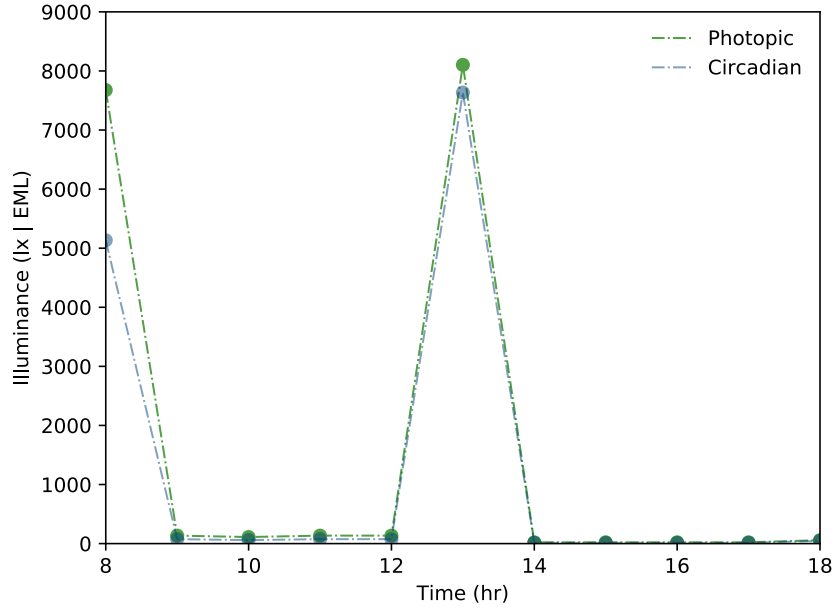
Figure 5.12. Variation of photopic and melanopic illuminance on Feb 25th with low circadian light

6. Accuracy Validation

Chapter 4 demonstrated the utilization of HDR photography along with tristimulus colorimeter calibration (CIE XYZ) to capture circadian light levels. The tristimulus color information is a data reduction of the actual wavelength based spectra. Accuracy of this methodology was tested through spectrophotometer measurements. The process and outcomes from this validation study is discussed here. Spectrophotometer measures spectral power distribution (SPD) for 400 values within visible wavelength (380nm – 780nm). The validation study is to test whether the calculated circadian light values from the CIE XYZ calibrated HDR photographs are in reasonable proximity to the calculated circadian measurements from the SPD measurements of the spectrophotometer.

6.1. Measurements

Further data has been collected over a period of two months where both SPD and CIE XYZ values were taken when capturing a HDR photograph, for a total of 33 indoor and outdoor scenes (Fig. 6.1.) . UPRtek MK350S Spectrophotometer was used to measure SPD of incident light and CIE XYZ values. Konica Minolta CL-200A illuminance color meter was also used to collect CIE XYZ values to check spectrophotometer's measurement consistency and reliability. Spectrophotometer was placed on top of the camera lens body with sensor facing towards the captured scene. Illuminance color meter was placed in front of the lens as in previous measurements. SPD was recorded in 1nm interval ranging from 380 to 780nm with maximum radiant power as 1. This normalized data was scaled according to the photometric measurements.
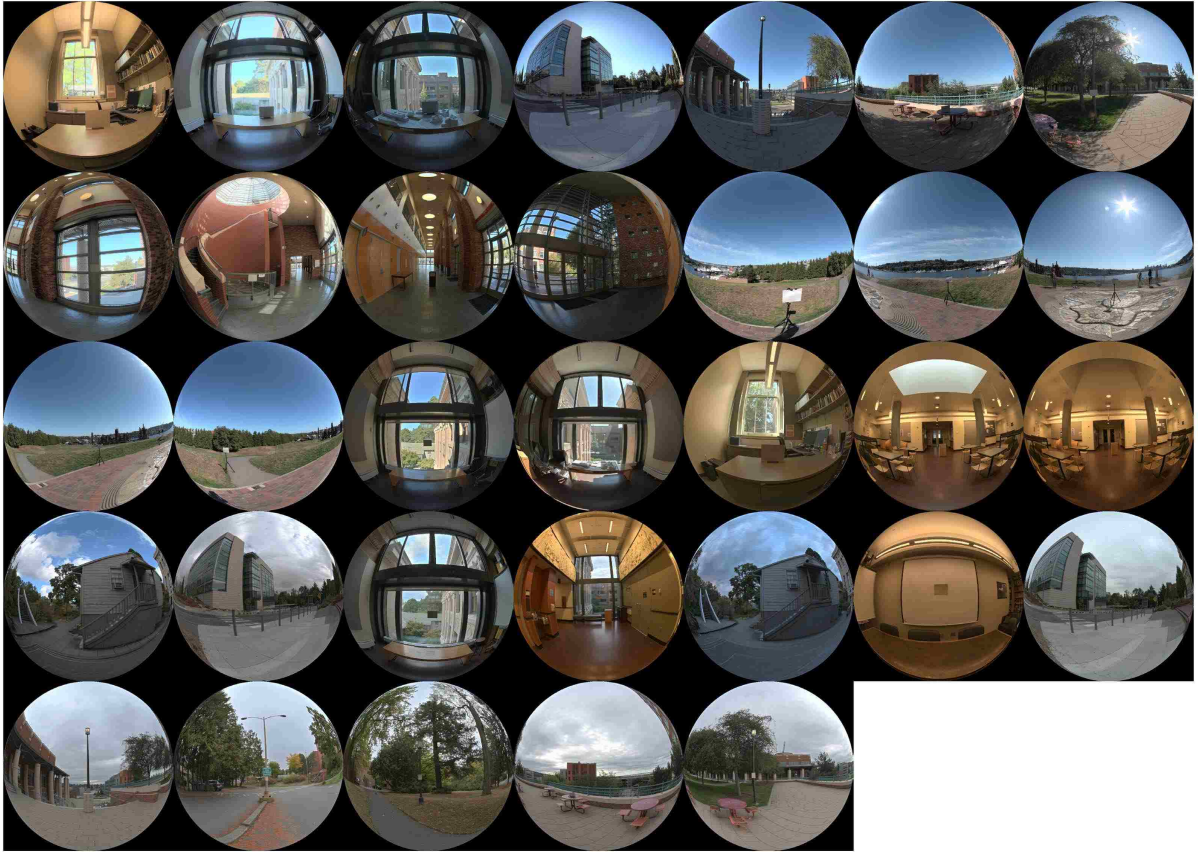
Figure 6.1. HDR photographs taken for validation study within various light conditions

6.2. Analysis

6.2.1. Measurement consistency between devices: Spectrophotometer and Color meter

As both UPRtek MK350S Spectrophotometer and Konica Minolta CL-200A illuminance color meter measures CIE XYZ, these values were compared for calibration accuracy of two devices. It should be noted even two scientific measurement devices (even from same manufacturer) can demonstrate inconsistency in measurements due to instrument calibration. Plotting CIE XYZ values from two devices showed linear correlation between measurements except for two cases

(Fig. 6.2.). These were accounted for measurement errors during data collection (angular discrepancies led to significant variation in field of view) and were excluded in calculating average percentage error. With this exclusion, mean percentage error between the measured values from two devices were around 9% for X, 10% for Y and 7% for Z measurements.

X

$y = 1.0155 \, x$

$r^2 = 0.98171$

Y

$y = 1.0291 \, x$

$r^2 = 0.98402$

Z

$y = 0.9552 \, x$

$r^2 = 0.98522$
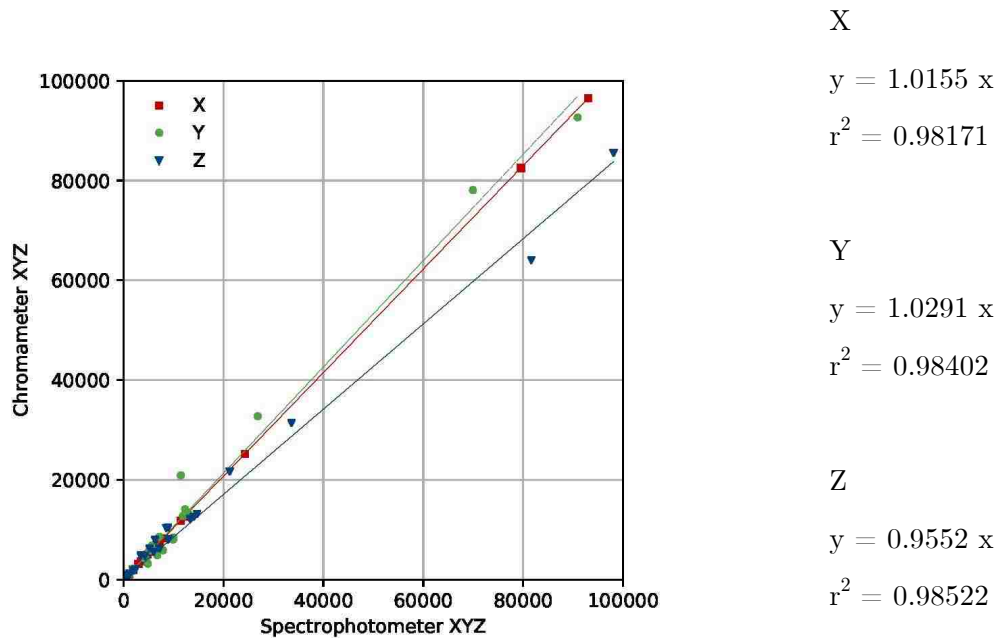
Figure 6.2. Comparison of measured CIE XYZ from spectrophotometer and illuminance color meter

6.2.2. Calculation Results from two measurements; SPD and CIE XYZ

For consistency in calculation method, HDR photos were calibrated with CIE XYZ values measured from the spectrophotometer. After post processing the HDR photos and calibrating RGB values, EML was calculated using the method described in section 4.3. Calculation process of EML from SPD is shown in figure 6.3. Two example scenes are shown in figure 6.4. Measured

spectral power distribution (SPD) clearly shows spectral difference between daylit and electric lit environments. Daylit environment in scene a) had much smoother curve for SPD while integrated electrical lighting in scene b) is much more erratic and peaks in certain parts of visible spectrum. This narrowly defined peaks can be especially important when calculating the EML values. Note that figure 6.4.b is the scene for the data shown in 6.3.
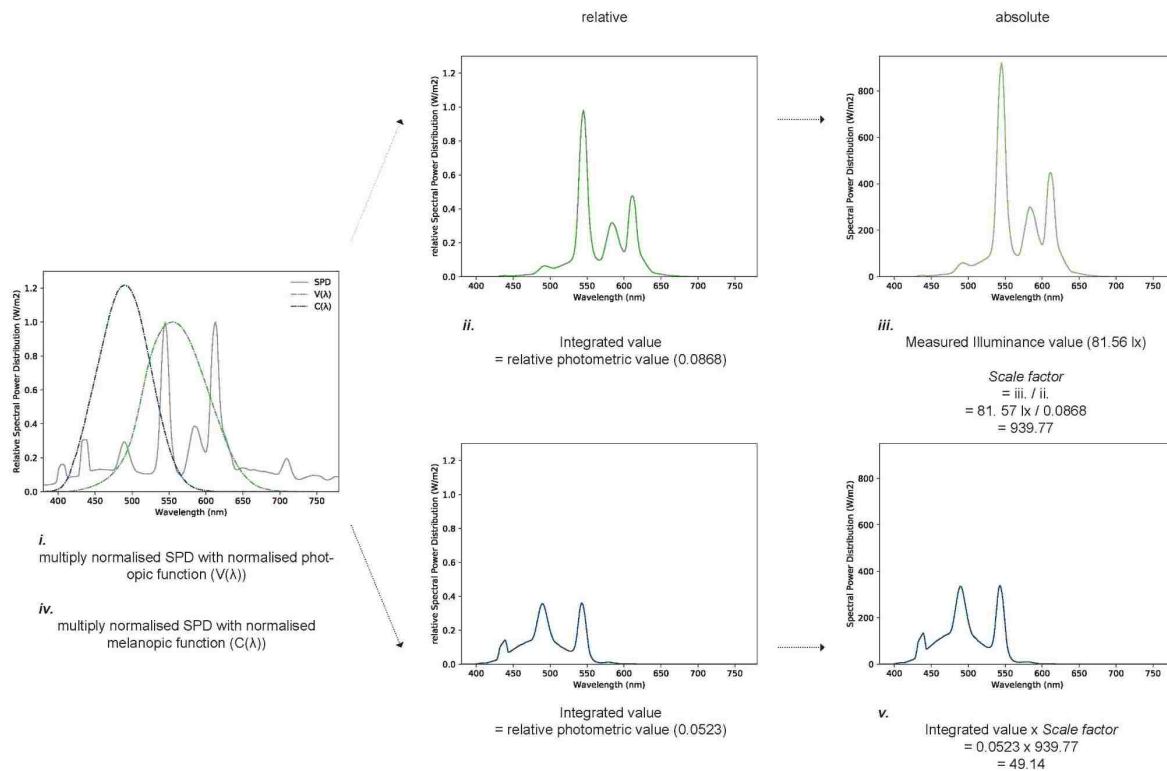
Figure 6.3. Calculation of EML from SPD. Process is as follows;

      i. Multiply normalized SPD with normalized photopic function ($V(\lambda)$) for each wavelength

      ii. Integrated value from resultant function is relative photopic value

      iii. This relative photopic value is multiplied by scale factor to match to measured illuminance value (This scale factor represents energy required to scale the relative photopic value to measured photometric value)

      iv. Multiply normalized SPD with normalized melanopic function ($C(\lambda)$) for each wavelength

      v. Integrated value from iv. is multiplied by π and scale factor

Scene HDR / Spectrum	Photopic	Circadian

(a) Sep 15 9:26 am

784 lx   555 lx

640 lx

(b) Oct 11 5:08 pm

87 lx   52 lx

49 lx

| 1 | 5 | 14 | 36 | 109 | 326 | 973 | 3000 | cd/m² |
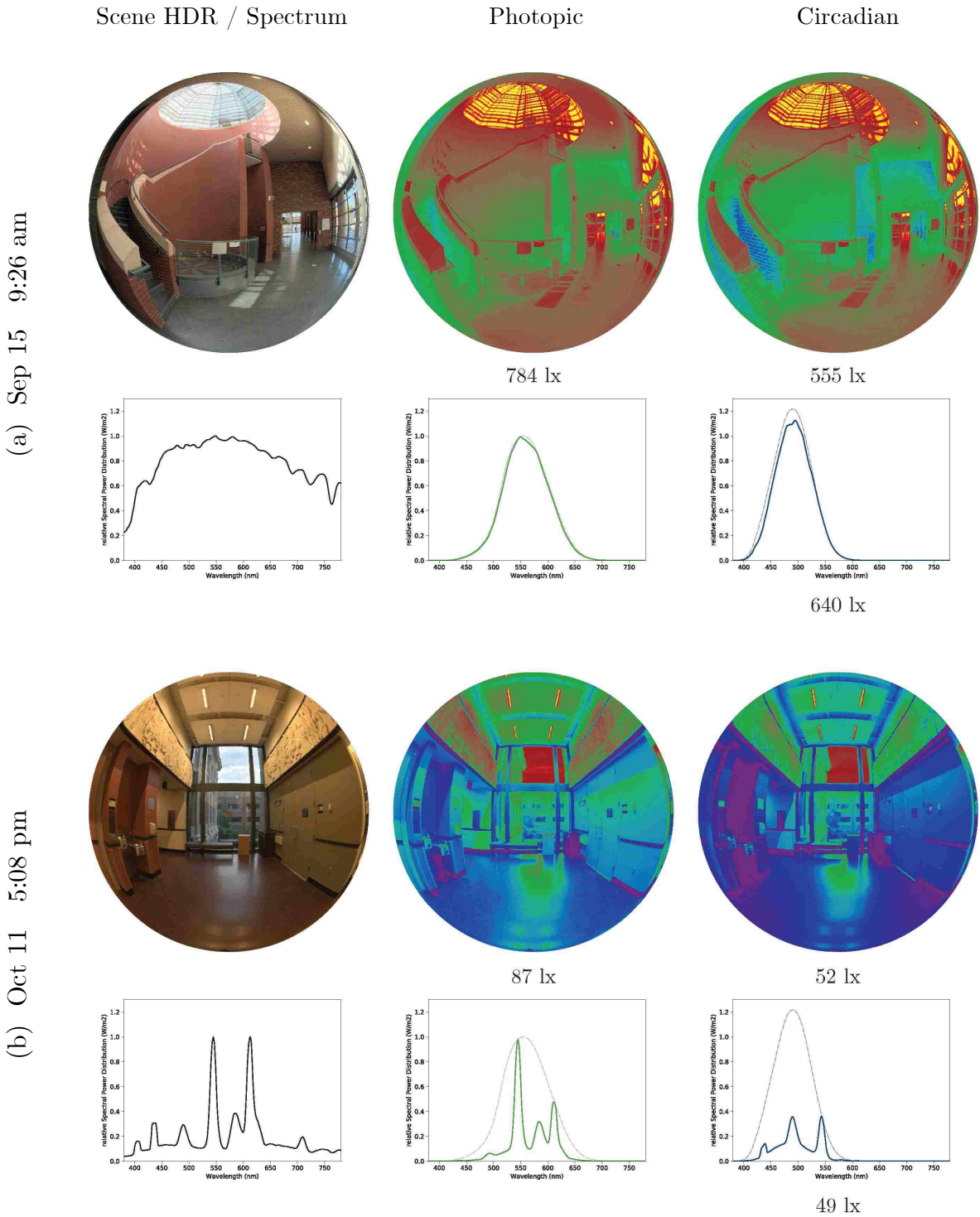
Figure 6.4. Calculated EML from full spectrum and HDR photographs

86

Plotting the calculated EML values from full spectrum and HDR photograph demonstrated that the results are quite similar. The results demonstrate that the tristimulus calibrated HDR photographs can measure EML values in close proximity to SPD derived EML values (Fig. 6.5). Small discrepancies between the two forms of measurements can be attributed for several reasons such as alignment of the devices in the field or the data reduction from 400 channels (1nm SPD) data to 3 channel measurements. Calculated average error was around 10% and the maximum error as 16%, aligning well with the accepted error rate of 20% in lighting simulations and physical measurements.
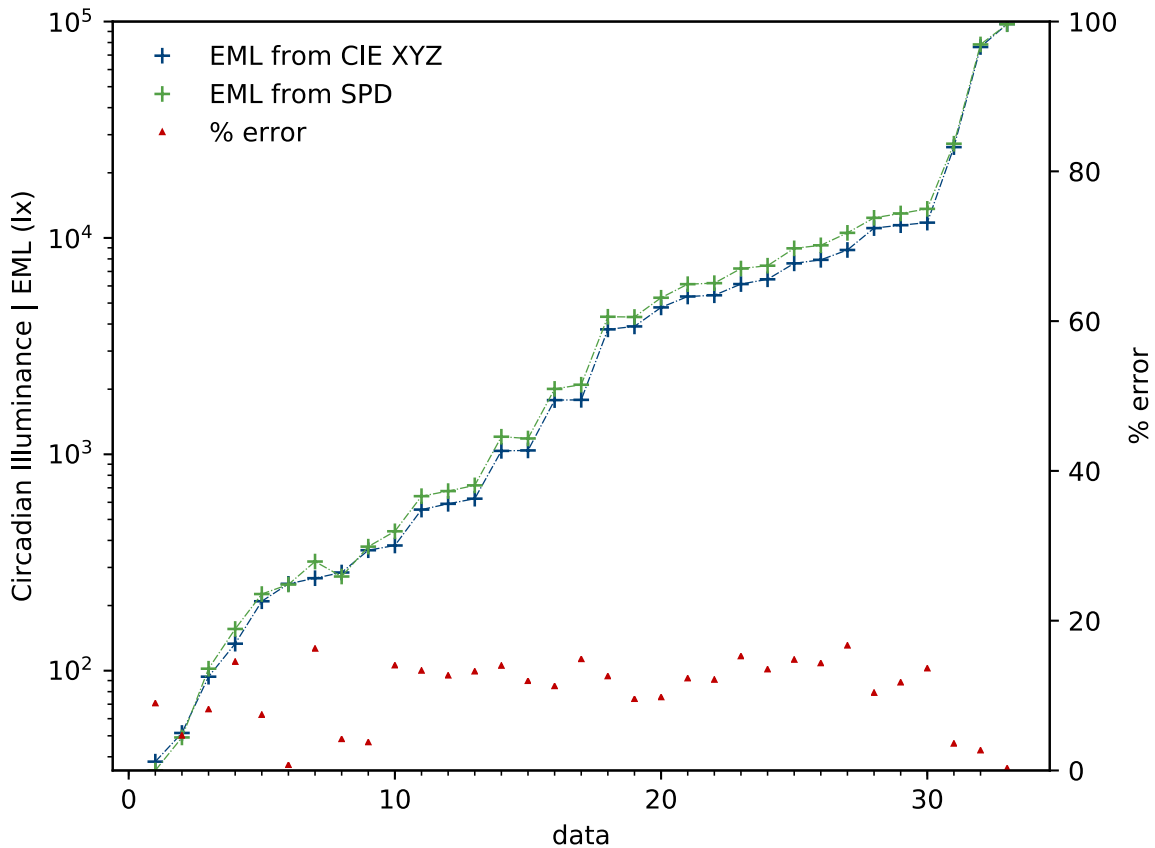
Figure 6.5. Variation of EML calculated from Full spectrum and HDR photographs

Average percentage error rate was around 10 % and maximum error around 16 %.

7. Conclusion

This thesis presents a framework for calibration and validation procedures for measuring circadian light through commercially available camera. The technique makes measuring circadian light accessible to all lighting professionals through HDR photography, allowing for rich collection data to gather information on current circadian light conditions within the luminous environment.

In chapter 2, biological background information on circadian system is discussed. ipRGCs are photoreceptors in the retina that has been recently discovered and research regarding its role is ongoing. ipRGCs are most sensitive to blue part of the visible spectrum due to a photopigment inside called melanopsin. It also registers light signals from not only the cell itself, but also from rods and cones (responsible for visible system). However, the direct relationship between these photoreceptors is not known. Due to this lack of scientific information, exact information on circadian entrainment is not known either. Research shows intensity, spectrum, duration, timing, photic history, spatial distribution and age all plays a role.

Background information on application of circadian rhythm within the built environment is explained in chapter 3. Much like the research on biological side, research within the built environment is on going and constantly evolving. A major concern is the lack of consensus on the physical form and scaling of the circadian sensitivity curve (circadian efficacy function). Without knowing how ipRGCs interacts with rods and cones, it is very difficult to define sensitivity of the

88

non-visual system through one sensitivity curve. Different curves has been introduced; trying to incorporate the function of ipRGCs, rods and cones into one function and separating the sensitivity curve for each photopigment within photoreceptors. Each of these curves has different scaling: scaling to have same integrated value and scaling to have same maximum value as the photopic curve. Circadian sensitivity curve called melanopic sensitivity function has been used in this study, scaled to have same area as the photopic curve.

In studying the circadian rhythm in built environments, simulation based research has been explored more than the physical measurements. Both point in time luminance analysis and annual (or periodic; month and week) illuminance analysis has been developed through numerous metrics. Research on circadian light through physical measurement has been limited as very few propriety devices exist, which are not widely available. Existing devices range in their ability to collect data. One device measures point in time luminance and another wearable device measures illuminance for a period of time.

Lack of physical measurement devices to measure circadian light within the luminous environments seriously impacts our understanding of the current conditions. Accessible measurement devices are needed to quickly gather large amount of data to develop guidelines and metrics for circadian friendly environments. Chapter 4 outlines the methodology for measuring circadian light through HDR photographs. HDR photographs for capturing photopic light has been validated in the past. To accurately capture circadian light, studying color accuracy of HDR photographs is the key as circadian efficacy function peaks at the blue part of the visible spectrum.

The chapter discusses process for capturing HDR photographs and post processing in detail. It also explains different metrics of measuring color in both physical and digital environments. Illuminance based color meter was used to measure color (CIE XYZ) in the physical environment, and images were calibrated with CIE XYZ. Plotting the measured tristimulus color values from the illuminance color meter, and the integrated response of the captured sRGB pixel values in cosine corrected 180° HDR photograph showed linear relationship. Green channel had almost 1 to 1 relation while red channel was underestimated and blue channel over estimated. Simple correction was applied to align the measured and captured data. This calibration coefficient was used to calibrate the color of camera sensors.

Chapter 5 illustrates some examples from captured HDR photographs, looking at both photopic and circadian illuminance in different light conditions and outlines some factors that affects circadian rhythm. Architectural context (form, spectral properties of building materials, surrounding urban and natural elements), spectra of light, weather, view direction and building depth all affects variability and quantity of circadian light levels. Intensity of light is much higher in outdoor environments. Lower levels of daylight within the built environments leads to lower circadian illuminance in general. However, the design decisions such as size and orientation of windows, spectral properties of glass, shading devices, opaque surface materials, and the electric light sources have significant impact on circadian lighting. Many design challenges remain within the built environment to improve lighting conditions for both photopic and circadian light. Holistic approach is required to develop lighting strategies appropriate for its context and variation of occupant's visual and circadian needs during different times of day and year. In relative color of

light described in CCT, approximately 6000°K was found as the threshold for raising circadian illuminance above photopic illuminance with identical intensity of light in studied scenes.

Finally, validation of the methodology is discussed in chapter 6. Further testing was done to test the accuracy of calculated EML values between the calculations from a CIE XYZ calibrated HDR photographs and full spectrum spectrophotometer measurements. EML results from full spectrum data and HDR photographs were compared. Results showed strong linear relationship with average of 10% error. Discrepancies between results can be attributed to alignment errors during field measurements and data reduction from full spectrum to 3 chromaticities.

It is important to note that the methodology also demonstrates how to calculate EML values from simple colorimeteric (CIE XYZ) measurements. Yet, using HDR photography (not just the CIE XYZ) measurements allows the user to capture the entire scene in a pixel scale, and therefore reveals the circadian distributions in the scenes (circadian luminance values in equivalent melanopic cd/m^2).

7.1. Contributions

Currently, most research regarding application of circadian light within the built environment has been performed in controlled laboratory environments due to lack of accessible measurement devices. The devices used in these labs does not measure circadian light and often ignores the impact of surrounding environments on circadian light exposure. Thus, variability and quantity of circadian light within the luminous environment is not well known. This study provides accessible and quick method of measuring circadian light to all lighting professionals.

HDR photography has the advantage of providing visual representations of an environment. This is particularly useful in studying different configuration of spaces and to visually understand which factors contribute to circadian light in complex architectural settings. HDR photography for photopic light has had deep impact in developing human centric metrics such as evaluation of glare. Similar outcome is expected for circadian light through rich collection of data. This thesis provided an accessible photography based technique to collect data to study the light and dark cycles of everyday life and should be used to develop metrics and guidelines for circadian friendly environments.

7.2. Future Work

This study provided calibration method and validation of HDR photography technique to measure circadian light through commercially available camera. However, only one camera make and model was used to develop the methodology. As explained previously in chapter 6, even individual devices of same make and model cannot have identical physical components for the sensors. Color calibration equations may be different for other cameras. Therefore, the methodology should be

replicated for other camera makes and models to test its color accuracy and calibration before measuring circadian light. Lighting researchers, designers and other professionals should replicate the methodology here for their individual cameras to derive the color calibration functions. Further studies with the same camera models and makes among different researchers could be compared whether color calibrations for the same camera make and model can be shared among users, or whether it should be generated for each camera.

Moreover, more biological and physiological case studies are required to develop guidelines. Development of a standardized circadian sensitivity function for the calculation of circadian light will reduce the confusion in metrics and enable users to compare data in a consistent manner. Guidelines on duration, intensity and timing of circadian light exposure for entrainment / disruption are also needed. These information is critical in developing appropriate metrics and guidelines for implementation in the built environment. The premise of this thesis is that an accessible circadian measurement device will help lighting professions to gather critical data to advance the understanding of the impact of built environments on circadian rhythms, and to make circadian friendly design decisions.

Bibliography

[1] Stevens, R.G., Brainard, G.C., Blask, D.E., Lockley, S.W., & Motta, M.E. (2013). Adverse Health Effects of Nighttime Lighting. *American Journal of Preventive Medicine 45*(3), 343–346.

[2] Blask, D.E., Brainard, G.C., Dauchy, R.T., Hanifin, J.P., Davidson, L.K., Krause, J.A.,...Zalatan, F. (2005). Melatonin-depleted blood from premenopausal women exposed to light at night stimulates growth of human breast cancer xenografts in nude rats. *Cancer Research, 65*(23), 11174-11184.

[3] McCurry, S.M., & Ancoli-Israel, S. (2003). Sleep dysfunction in alzheimer's disease and other dementias, *Current Treatment Options in Neurology, 5*(3), 261-272.

[4] Desimone, R. (1991). Face-selective cells in the temporal cortex of monkeys, *Journal of Cognitive Neuroscience, 3*, 1–8.

[5] Boyce, P.R. (2003). *Human Factors in Lighting, Second Edition.* London: Taylor and Francis Group.

[6] Berson, D.M., Dunn, F.A., & Montoharu, T. (2002). phototransduction by retinal ganglion cells that set the circadian clock. *Science, 295,* 1070–1073.

[7] Hattar, S. Liao, H.W., Takao, M., Berson, D.M., & Yau, K.W. (2002). Melanopsin-containing retinal ganglion cells: architecture, projections, and intrinsic photosensitivity, *Science, 295,* 1065–1070.

[8] Adler, J.S., Kripke, D.F., Loving, R.T., & Berga, S.L. (1992). Peripheral vision suppression of melatonin, *Journal of Pineal Research, 12,* 49–52.

[9] Lasko, T.A., Kripke, D.F., & Elliot, J.A. (1999). Melatonin suppression by illumination of upper and lower visual fields. *Journal of Biological Rhythms, 14,* 122–125.

[10] Pu, M. (2000). Physiological response properties of the cat retinal ganglion cells projecting to the suprachiasmatic nucleus, *Journal of Biological Rhythms, 15,* 31–6.

[11] Enezi, J.A., Revell, V., Brown, T., Wynne, J., Schlangen, L., & Lucas, R. (2011). A "Melanopic" Spectral Efficiency Function Predicts the Sensitivity of Melanopsin Photoreceptors to Polychromatic Lights. *Journal of Biological Rhythms, 26*(4), 314-323.

[12] Moore, R.Y., Speh, J.C., & Card, J.P. (1995). The reinohypothalamic tract originates from a distinct subset of retinal ganglion cells. *The Journal of Comparative Neurology, 352*(3), 351-366.

[13] Groos, G.A. & Mason, R. (1980). The visual properties of rat and cat suprachiasmatic neurones, *Journal of Comparative Physiology A, 135,* 349–56.

[14] Ebihara, S., & Tsuji, K. (1980). Entrainment of the circadian activity rhythm to the light cycle: effective light intensity for a Zeitgeber in the retinal degenerate C3H mouse and the normal C57BL mouse. *Physiology & Behavior, 24,* 523–527.

[15] Lucas, R.J. (2012). Mammalian Inner Retinal Photoreception. *Current Biology. 23*(3), 125–133.

[16] DiLaura, D.I., Houser, K.W., Mistrick, R.G., & Steffy, G.R. (2011). *IES The Lighting Handbook Tenth Edition Reference and Application.* New York, NY: IESNA.

[17] Provencio, I., & Foster, R. (1995). Circadian rhythms in mice can be regulated by photoreceptors with cone-like characteristics, *Brain Research, 694,* 183–190.

[18] Foster, R.G., Argamaso, S., Coleman, S., Colwell, C.S., Lederman, A., & Provencio, I. (1993). Photoreceptors regulating circadian behavior: A mouse model, *Journal of Biological Rhythms, 8,* 17–23.

[19] Yoshimura, T., & Ebihara, S. (1996). Spectral sensitivity of photoreceptors mediating phase-shifts of circadian rhythms in retinally degenerate CBA/J (rd/rd) and normal CBA/N (+/+)mice, *Journal of Comparative Physiology A, 178,* 797–802.

[20] Czeisler, C.A., Shanahan, T.L., Klerman, E.B., Martens, H., Brotman, D.J., Emens, J.S., ... Rizzo, J.F. (1995). Suppression of melatonin secretion in some blind patients by exposure to bright light, *New England Journal of Medicine, 332,* 6–11.

[21] Freedman, M.S., Lucas, R.J., Soni, B., von Schantz, M., Munoz, M., David-Gray, Z., & Foster, R.G. (1999). Regulation of mammalian circadian behavior by non-rod, non-cone, ocular photoreceptors, *Science, 284,* 502–504.

[22] Lucas, R.J., Freedman, M.S., Munoz, M., Garcia-Fernandez, J.M., & Foster, R.G. (1999). Regulation of the mammalian pineal by non-rod, non-cone, ocular photoreceptors, *Science, 284* 505–507.

[23] Mrosovsky, N., Lucas, R., & Foster, R. (2001). Persistence of masking responses to light in mice lacking rods and cones, *Journal of Biological Rhythms, 16,* 585–587.

[24] Lucas, R., Douglas, R. & Foster, R. (2001). Characterization of an ocular photopigment capable of driving pupillary constriction in mice, *Nature Neuroscience, 4,* 621–626.

[25] Belenky, M.A., Smeraski, C.A., Provencio, I., Sollars, P.J., & Pickard, G.E. (2003). Melanopsin retinal ganglion cells receive bipolar and amacrine cell synapses, *Journal of Comparative Physiology, 460,* 380–393.

[26] Dumitrescu, O.N., Pucci, F.G., Wong, K.Y., & Berson, D.M. (2009). Ectopic retinal ON bipolar cell synapses in the OFF inner plexiform layer: contacts with dopaminergic amacrine cells and melanopsin ganglion cells, *Journal of Comparative Physiology, 517,* 226–244.

[27] Hoshi, H. Liu, W.L., Massey, S.C., & Mills, S.L. (2009). ON inputs to the OFF layer: bipolar cells that break the stratification rules of the retina, *Journal of Neuroscience, 29,* 8875–8883.

[28] Viney, T.J., Balint, K., Hillier, D. Siegert, S., Boldogkoi, Z.,...Roska, B. (2007). Local retinal circuits of melanopsin-containing ganglion cells identified by transsynaptic viral tracing, *Current Biology, 17,* 981–988.

[29] Ostergaard, J., Hannibal, J., & Fahrenkrug, J. (2007). Synaptic contact between melanopsin-containing retinal ganglion cells and rod bipolar cells, *Investigative ophthalmology and visual science, 48,* 3812–3820.

[30] Lucas, R.J., Hattar, S., Takao, M., Berson, D.M., Foster, R.G., & Yau, K.W. (2003) Diminished pupillary light reflex at high irradiances in melanopsin-knockout mice, *Science, 299,* 245–247.

[31] Panda, S., Sato, T.K., Castrucci, A.M., Rollag, M.D., DeGrip, W.J., Hogenesch, J.B.,...Kay, S.A. (2002). Melanopsin (Opn4) requirement for normal light-induced circadian phase shifting, *Science, 298,* 2213–2216.

[32] Ruby, N.F., Brennan, T.J., Xie, X., Cao, V., Franken, P., Heller, H.C., & O'Hara, B.F. (2002). Role of melanopsin in circadian responses to light, *Science, 298,* 2211–2213.

[33] Hattar, S., Lucas, R.J., Mrosovsky, N., Thompson, S., Douglas, R.H., Hankins, M.W.,...Yau, K.W. (2003). Melanopsin and rod-cone photoreceptive systems account for all major accessory visual functions in mice, *Nature, 424,* 75–81.

[34] Panda, S., Provencio, I., Tu, D.C., Pires, S.S., Rollag, M.D., Castrucci, A.M.,...Hogenesch, J.B. (2003). Melanopsin is required for non-image-forming photic responses in blind mice, *Science, 301,* 525–527.

[35] Guler, A.D., Ecker, J.L., Lall, G.S., Haq, S., Altimus, C.M., Liao, H.W.,...Hattar, S. (2008). Melanopsin cells are the principal conduits for rod-cone input to non-image-forming vision, *Nature, 453,* 102–105.

[36] Hatori, M., Le, H., Vollmers, C., Keding, S.R., Tanaka, N., Schmedt, C.,...Panda, S. (2008). Inducible ablation of melanopsin-expressing retinal ganglion cells reveals their central role in non-image forming visual responses, *PLoS ONE, 3,* e2451.

[37] Goz, D., Studholme, K., Lappi, D.A., Rollag, M.D., Provencio, I., & Morin, L.P. (2008) Targeted destruction of photosensitive retinal ganglion cells with a saporin conjugate alters the effects of light on mouse circadian rhythms, *PLoS ONE, 3*(6), e3153.

[38] Lucas, R.J., Peirson, S., Berson, D.M., Brown, T.M., Cooper, H.M., Czeisler, C.A.,...Brainard, G.C. (2014). Measuring and using light in the melanopsin age. *Trends in Neurosciences 37*(1), 1-9.

[39] Dacey, D.M., Liao, H.W., Peterson, B.B., Robinson, F.R., Smith, V.C., Pokorny, J.,...Gamlin, P.D. (2005). Melanopsin-expressing ganglion cells in primate retina signal color and irradiance and project to the LGN, *Nature, 433,* 749–754.

[40] Perez-Leon, J.A., Warren, E.J., Allen, C.N., Robinson, D.W., & Lane Brown, R. (2006). Synaptic inputs to retinal ganglion cells that set the circadian clock, *European Journal of Neuroscience, 24,* 1117–1123.

[41] Brown, T.M., Gias, C., Hatori, M., Keding, S.R., Semo, M., Coffey, P.,...Lucas, R.J. (2010). Melanopsin contributions to irradiance coding in the thalamo-cortical visual system, *PLOS Biology., 8*(12), e1000558.

[42] Mure, L.S., Rieux, C., Hattar, S., & Cooper, H.M. (2007). Melanopsin-dependent nonvisual responses: evidence for photopigment bistability in vivo, *Journal of Biological Rhythms, 22,* 411–424.

[43] Gooley, J.J., Rajaratnam, S.M., Brainard, G.C., Kronauer, R.E., Czeisler, C.A., & Lockley, S.W. (2010). Spectral responses of the human circadian system depend on the irradiance and duration of exposure to light, *Science Translational Medicine, 2*(31), 31-33.

[44] Gamlin, P.D., McDougal, D.H., Pokorny, J., Smith, V.C., Yau, K.W., & Dacey, D.M. (2007) Human and macaque pupil responses driven by melanopsin-containing retinal ganglion cells, *Vision Research, 47,* 946–954.

[45] Altimus, C.M., Guler, A.D., Alam, N.M., Arman, A.C., Prusky, G.T., Sampath, A.P., & Hattar, S. (2010). Rod photoreceptors drive circadian photoentrainment across a wide range of light intensities, *Nature Neuroscience, 13,* 1107–1112.

[46] Schmidt, T.M., Taniguchi, K., & Kofuji, P. (2008) Intrinsic and extrinsic light responses in melanopsin-expressing ganglion cells during mouse development. *J. Neurophysiol., 100*(1), 371-384

[47] Lucas, R.J., Lall, G.S., Allen, A.E., & Brown, T.M. (2012). How rod, cone, and melanopsin photoreceptors come together to enlighten the mammalian circadian clock. *Progress in Brain Research. 199,* 1–18.

[48] Glickman, G., Levin, R., & Brainard, G.C. (2002). Ocular input for human melatonin regulation: relevance to breast cancer. *Neuroendocrinology Letters, 23*(2), 17–22.

[49] McDougal, D.H. & Gamlin, P.D. (2010). The influence of intrinsically- photosensitive retinal ganglion cells on the spectral sensitivity and response dynamics of the human pupillary light reflex. *Vision Research. 50*(1), 72–87.

[50] Kankipati, L., Girkin, C.A., & Gamlin, P.D. (2010). Post-illumination pupil response in subjects without ocular disease. *Investigative Ophthalmology and Visual Science. 51*, 2764–2769.

[51] Allen, A.E., Brown, T.M., & Lucas, R.J. (2011). A distinct contribution of short-wavelength-sensitive cones to light-evoked activity in the mouse pretectal olivary nucleus. *Journal of Neuroscience, 31*(46), 16833–16843.

[52] Brown, T.M., Wynne, J., Piggins, H.D., & Lucas, R.J. (2011). Multiple hypothalamic cell populations encoding distinct visual information. *Journal of Physiology, 589*(5), 1173–1194.

[53] Ecker, J.L., Dumitrescu, O.N., Wong, K.Y., Alam, N.M., Chen, S.K., LeGates, T.,...Hatter, S. (2010). Melanopsin-expressing retinal ganglion-cell photoreceptors: cellular diversity and role in pattern vision. *Neuron 67*(1), 49–60.

[54] Rea, M.S., Figueiro M.G., Bullough, J.D., & Bierman, A. (2005). A model of phototransduction by the human circadian system. *Brain Research Reviews. 50*(1), 213–228.

[55] Amundadottir, M.L., St. Hilaire, M.A., Lockley, S.W., & Andersen, M. (2013). Unifying spectral sensitivity and temporal characteristics in a single model structure, Proceedings from CIE Centenary Conference: *Towards a New Century of Light Modeling non-visual responses to light.* Apr 15-16, Paris, France.

[56] Brainard, G.C., Hanifin, J.R., Greeson, J.M., Byrne, B., Glickman, G., Gerner, E., & Rollag, M.D. (2001). Action spectrum for melatonin regulation in humans: evidence for a novel circadian photoreceptor. *Journal of Neuroscience. 21*(16), 6405–6412.

[57] Thapan, K., Arendt, J., & Skene, D.J. (2001). An action spectrum for melatonin suppression: evidence for a novel non-rod, non-cone photoreceptor system in humans. *Journal of Physiology. 535*(1), 261–267.

[58] Gall, D. & Beiske, K. (2004). Definition and measurement of circadian radiometric quantities, Proceedings from *CIE Symposium '04*, Sep 30–Oct 2, Vienna, Austria.

[59] Foster, R.G. & Hankins, M.W. (2002). Non-rod, non-cone photoreception in the vertebrates. *Progress in Retinal and Eye Research, 21*(6), 507-527.

[60] Hankins, M.W. & Lucas, R.J. (2002). The primary visual pathway in humans is regulated according to long-term light exposure through the action of a nonclassical photopigment. *Current Biology, 12*(3), 191-198.

[61] Cajochen, C., Kräuchi, K., & Wirz-Justice, A. (2003). Role of Melatonin in the Regulation of Human Circadian Rhythms and Sleep, *Journal of neuroendocrinology, 15*(4), 432–437.

[62] Reiter, R.J., Tan, D.X., Manchester, L.C., Paredes, S.D., Mayo, J.C., & Sainz, R.M. (2009). Melatonin and reproduction revisited, *Biology of Reproduction, 81*(3), 445-56.

[63] Tan, D.X., Chen, L.D., Poeggeler, B., Manchester, L.C., & Reiter, R.J. (1993). Melatonin: a potent, endogenous hydroxyl radical scavenger, *Endocrine Journal, 738*, 57–60.

[64] Carrillo-Vico, A., Guerrero, J.M., Lardone, P.J., & Reiter, R.J. (2005). A review of the multiple actions of melatonin on the immune system, *Endocrine, 27*(2), 189-200.

[65] Czeisler, C.A., Duffy, J.F., Shanahan, T.L., Brown, E.N., Mitchell, J.F., Rimmer, D.W.,...Kronauer, R.E. (1999). Stability, Precision, and Near-24-Hour Period of the Human Circadian Pacemaker, *Science, 284*, 2177-2181.

[66] Konis, K. (2017). A novel circadian daylight metric for building design and evaluation. *Building and Environment, 113*, 22-38.

[67] Wright Jr, K.P., McHill, A.W., Birks, B.R., Griffin, B.R., Rusterholz, T., & Chinoy, E.D. (2013). Entrainment of the Human Circadian Clock to the Natural Light Dark Cycle, *Current Biology, 23*(16), 1554-1558.

[68] Zeitzer, J.M., Dijk, D.J., Kronauer, R.E., Brown, E.N., & Czeisler, C.A. (2000). Sensitivity of the human circadian pacemaker to nocturnal light: melatonin phase resetting and suppression. *The Journal of Physiology, 526*(3), 695–702.

[69] Cajochen, C., Zeitzer, J.M., Czeisler, C.A., & Dijk, D.J. (2000). Dose-response relationship for light intensity and ocular and electroencephalographic correlates of human alertness. *Behavioural Brain Research, 115*(1), 75-83.

[70] WELL Building Standard. (2014) *WELL Building Standard (v1).* International Well Building Institute.

[71] Chang, A.M., Santhi, N., St Hilaire, M., Gronfier, C., Bradstreet, D.S., Duffy, J.F.,...Czeisler, C.A. (2012). Human responses to bright light of different durations. *Journal of Physiology, 590*(13), 3103-3012.

[72] Reiter, R.J. (1985). Action spectra, dose-response relationships, and temporal aspects of light's effects on the pineal gland. *Ann. NY Acad. Sci. 453*, 215–30.

[73] Lewy, A.J., Wehr, T.A., Goodwin, F.K., Newsome, D.A., & Markey, S.P. (1980). Light suppresses melatonin secretion in humans. *Science, 210*, 1267– 69.

[74] McIntyre, I.M., Norman, T.R., Burrows, G.D., & Armstrong, S.M. (1989) Human melatonin suppression by light is intensity dependent. *J. Pineal Res, 6(2)*, 149–56.

[75] Rea, M.S., Figueiro M.G., & Bullough, J.D. (2002). Circadian photobiology: An emerging framework for lighting practice and research. *Lighting Research Technology, 34*(3). 177-187.

[76] McIntyre, I.M., Norman, T.R., Burrows, G.D., & Armstrong, S.M. (1989) Quantal melatonin suppression by exposure to low intensity light in man. *Life Sci, 45*(4), 327–32.

[77] Wong, K.Y., Dunn, F.A., & Berson, D.M. (2005). Photoreceptor adaptation in intrinsically photosensitive retinal ganglion cells. *Neuron. 48*(6), 1001-10.

[78] Hébert, M., Martin, S.K., Lee, C., & Eastman, C.I. (2002). The effects of prior light history on the suppression of melatonin by light in humans. *J Pineal Res. 33*(4), 198-203.

[79] Smith, K.A., Schoen, M.W., & Czeisler, C.A. (2004). Adaptation of human pineal melatonin suppression by recent photic history. *J Clin Endocrinol Metab, 89*(7), 3610-4.

[80] Jasser, S.A., Hanifin, J.P., Rollag, M.D., & Brainard, G.C. (2006). Dim light adaptation attenuates acute melatonin suppression in humans. *J Biol Rhythms, 21*(5), 394-404.

[81] Chang, A.M., Scheer, F.A.J.L., & Czeisler, C. (2011). The human circadian system adapts to prior photic history, *J Physiol. 589*(5), 1095–1102.

[82] Kelpeis, N.E., Nelson, W.C., Ott, W.R., Robinson, J.P., Tsang, A.M., Switzer, P.,... Engelmann, W.H. (2001). The National Human Activity Pattern Survey (NHAPS): a resource for assessing exposure to environmental pollutants. *Journal of Exposure Analysis and Environmental Epidemiology, 11*(3), 231–252.

[83] Pechacek, C.S., Andersen, M., & Lockley, S.W. (2008). Prospective evaluation of the Circadian Efficacy of (Day)Light in Rooms. *Leukos, the Journal of the Illuminating Engineering Society, 5*(1), 1-26.

[84] Andersen, M., Mardaljevic, J., & Lockley, S.W. (2012). A framework for predicting the non-visual effects of daylight – Part I: photobiology- based model. *Lighting Research and Technology, 44*(1), 37-53.

[85] Phipps-Nelson, J., Redman, J., Dijk, D., & Rajaratnam, S. (2003). Daytime exposure to bright light, as compared to dim light, decreases sleepiness and improves psychomotor vigilance performance. *Sleep, 26*(6), 583–588.

[86] Mardaljevic, J., Andersen, M., Roy, N., & Christoffersen, J. (2013). A framework for predicting the non-visual effects of daylight – Part II: The simulation model. *Lighting Research and Technology, 46*(4), 388-406.

[87] Amundadottir, M.L., Lockley, S.W., & Andersen, M. (2013). Simulation-based Evaluation of Non-Visual Responses to Daylight: Proof of Concept Study of Healthcare Re-design. Proceedings of *13th IBPSA Conference*, Chambery, France.

[88] Inanici, M., Brennan, M., & Clark, E. (2015). Spectral Daylighting Simulations: Computing Circadian Light Proceedings of *14th IBPSA Conference*, Hyderabad, India.

[89] Rea, M.S. (2015). The lumen seen in a New Light: Making Distinctions between light, lighting, and Neuroscience. *Lighting Research and Technology, 47(3)*, 259-280.

[90] Amundadottir, M.L., Lockley, S.W., & Andersen, M. (2016). Unified framework to evaluate non-visual spectral effectiveness of light for human health. *Lighting Research and Technology, 49*, 1-24.

[91] Rea, M.S., Figueiro, M.G., Bierman, A., & Bullough, J.D. (2010). Circadian light, *Journal of Circadian Rhythms, 8*(2).

[92] Figueiro, M.G., Gonzales, K., & Pedler, D.R. (2016, October). Designing with Circadian Stimulus. Lighting Design and Applications. *The magazine of the IESNA (LD+A).* 30-34.

[93] Reinhart, C. Daysim [https://daysim.ning.com/]

[94] Reinhart, C.F., Mardaljevic, J., Rogers, Z. (2006). Dynamic Daylight Performance Metrics for Sustainable Building Design. *LEUKOS, 3*(1), 7-31

[95] Larson, G.W., Shakespeare, R.A. (2011). *Rendering with Radiance: The Art and Science of Lighting Visualization.* San Francisco, CA: Morgan Kaufmann.

[96] Borisuit, A., Kampf, J., Munch, M., Thanachareonkit, A., & Scartezzini, J.L. (2016). Monitoring and rendering of visual and photo-biological properties of daylight-redirecting systems. *Solar Energy, 129*, 297–309.

[97] Ruppertsberg, A.I., & Bloj, M. (2006) Rendering complex scenes for psychophysics using RADIANCE: How accurate can you get?, *Optical society of America*, 23(4), 759-768.

[98] Ruppertsberg, A.I., & Bloj, M. (2008) Creating physically accurate visual stimuli for free: Spectral rendering with RADIANCE, *Behavior Research Methods*, 40(1), 304-308.

[99] Bierman, A., Klein, T.R., & Rea, M.S., The Daysimeter: A device for measuring optical radiation as a stimulus for the human circadian system. *Measurement Science and Technology, 16*, 2292-2299.

[100] Lighting Research Center. (2011). Dimensimeter – Light and Activity Measurement System Description and Calibration. Retrieved from http://www.lrc.rpi.edu/programs/lightHealth/pdf/DimesimeterDoc.pdf

[101] Borisuit, A., Deschamps, L., Kampf, J., Scartezzini, J.L., & Munch, M. (2013). Assessment of circadian weighted radiance distribution using a camera-like light sensor. Proceedings of *CISBAT*. Lausanne, Switzerland.

[102] Borisuit, A., Munch, M., Deschamps, L., Kampf, J., & Scartezzini, J.L. (2012). A new device for dynamic luminance mapping and glare assessment in buildings. Proceedings of the *SPIE 2012 Optics + Photonics Conference*. San Diego, CA.

[103] Commission Internationale de L'Eclairage. (1987). CIE 069-1987: Methods of characterizing illuminance meters and luminance meters: Performance, characteristics and specifications, Vienna: CIE Central bureau.

[104] Miller, D., Bierman, A., Figueiro, M., Schernhammer, E., & Rea, M. (2010). Ecological measurements of light exposure, activity, and circadian disruption. *Lighting Research and Technology, 42*(3), 271–284.

[105] Inanici, M.N. (2006) Evaluation of high dynamic range photography as a luminance data acquisition system. *Lighting Res. Technol. 38*(2), 123-136.

[106] Jakubiec A, van den Wymelenberg K, Inanici M, & Mahic A. (2016). Accurate Measurement of Daylit Interior Scenes using High Dynamic Range Photography. *CIE 2016 Lighting Quality and Energy Efficiency Conference*, Melbourne, Australia.

[107] Inanici, M., & Jakubiec, A. (2016, July). Introduction to HDR Photography. Workshop presented at the 32nd International Conference on PLEA, Los Angeles, CA.

[108] Jakubiec A, van den Wymelenberg K, Inanici M, & Mahic A. (2016). Improving the Accuracy of Measurements in Daylit Interior Scenes using High Dynamic Range Photography. Proceedings from *PLEA 2016 Conference*, Los Angeles, CA.

[109] McCamy, C.S. (1992). Correlated color temperature as an explicit function of chromaticity coordinates. *Color Research and Application. 17*(2), 142-144.

[110] Ward G. Photosphere. [http://www.anyhere.com/]

[111] Mitsunaga, T., & Nayar, S.K. (1999). Radiometric self calibration, Proceedings of IEEE *Conference on Computer Vision and Pattern Recognition*. Fort Collins, CO.

[112] Kumaragurubaran, V., & Inanici, M. (2013). hdrscope: High Dynamic Range Image Processing Toolkit for Lighting Simulations and Analysis, Proceedings of *BS2013 13th Conference of International Building Performance Simulation Association*, Chambery, France.

[113] Wright, W.D. (1928). A re-determination of the trichromatic coefficients of the spectral colors, *Transactions of the Optical Society. 30*(4), 141–164.

[114] Guild, J. (1932). The colorimetric properties of the spectrum. *Philosophical Transactions of the Royal Society of London A, 230*, 149–187.

[115] Wyszecki, G., & Stiles, W.S. (2000) *Color Science: Concepts and Methods, Quantitative Data and Formulae, 2nd Edition.* New York, NY: John Wiley & Sons.

[116] Berns, R.S. (2000) Billmeyer and Saltzman's Principles of Color Technology, 3rd Edition. New York, NY : John Wiley & Sons.

[117] International Electrotechnical Commission. (1999) *Multimedia systems and equipment - Color measurement and management - Part 2-1: Color management - Default RGB color space - sRGB.* IEC 61966-2-1.

[119] Martha, P.M Jr., Gorman, K.M., Blizzard, R.M., Rogol, A.D., & Veldhuis, J.D. (1992). Endogenous growth hormone secretion and clearance rates in normal boys, as determined by deconvolution analysis: relationship to age, pubertal status and body mass. *J Clin Endocrinol Metab 74*(2), 336-44.